UCLouvain
Institute of Mechanics,
Materials and Civil Engineering

Robust optimisation of the pathway towards a sustainable whole-energy system

A hierarchical multi-objective reinforcement-learning based approach

Doctoral dissertation presented by
Xavier RIXHON

in partial fulfillment of the requirements for
the degree of Doctor in Engineering Sciences

December 2023

Thesis committee
Pr. Francesco CONTINO (supervisor, UCLouvain)
Pr. Hervé JEANMART (supervisor, UCLouvain)
Dr. Stefano MORET (ETH Zurich)
Pr. Sylvain QUOILIN (ULiège)

Contents

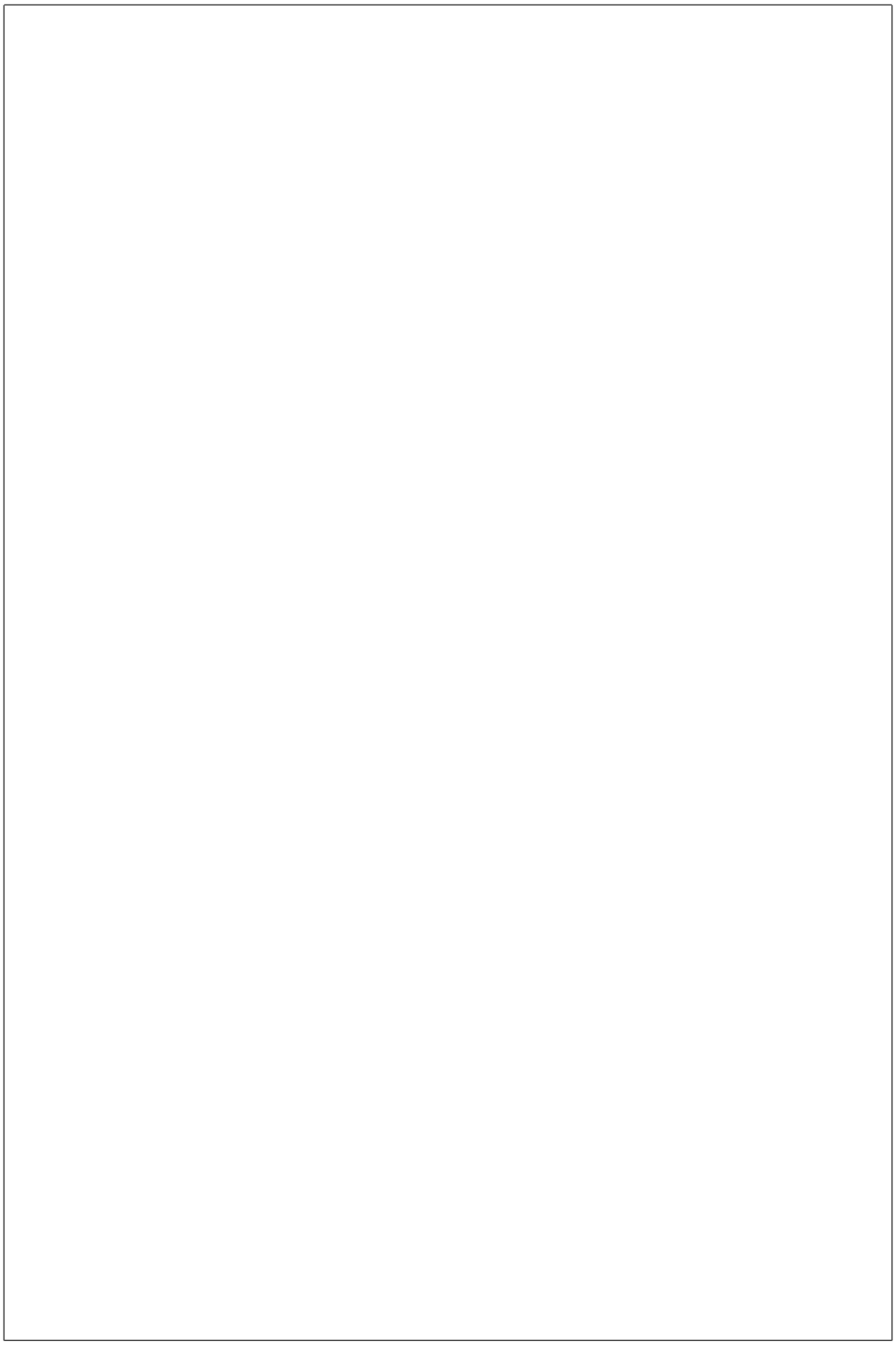

Symbols

Acronyms

API	application programming interface
BECCS	bioenergy with carbon capture and storage
BEV	battery electric vehicle
BTX	benzene, toluene and xylene
CAPEX	capital expenditure
CCGT	combined cycle gas turbine
CCS	carbon capture and storage
CHP	combined heat and power
CNG	compressed natural gas
DC	direct current
DHN	district heating network
ESOMs	energy system optimisation models
EnergyScope TD	EnergyScope Typical Days
EUD	end-use demand
FC	fuel cell
GDP	gross domestic product
GHG	greenhouse gases
GSA	global sensitivity analysis
GWP	global warming potential
HP	heat pump
HT	high-temperature
HVC	high value chemicals
ICE	internal combustion engine
IEA	International Energy Agency
IPCC	intergovernmental panel on climate change

IQR	interquatile range
LCA	life cycle assessment
LCOE	levelised cost of energy
LFO	light fuel oil
LOO	leave-one-out
LPG	liquefied petroleum gas
LT	low-temperature
MDP	Markov decision process
MMSA	Methanol Market Services Asia
MTBE	methyl tert-butyl ether
MTO	methanol-to-olefins
NED	non-energy demand
NG	fossil gas
NN	neural network
NRE	non-renewable energy
NSC	naphtha steam cracker
OPEX	operational expenditure
PC	principal component
PCA	Principal Component Analysis
PCE	Polynomial Chaos Expansion
PDF	probability density function
PV	photovoltaic
RE	renewable energy
RL	reinforcement learning
SAC	Soft Actor Critic
SDGs	Sustainable Development Goals
SMR	small modular reactor
SVD	singular value decomposition
UQ	Uncertainty Quantification
VRES	variable renewable energy sources

List of publications

Limpens, G., **Rixhon, X.**, Contino, F., & Jeanmart, H. (2024). "*EnergyScope Pathway: An open-source model to optimise the energy transition pathways of a regional whole-energy system.*" In Applied Energy, (Vol. 358). URL: `https://doi.org/10.1016/j.apenergy.2023.122501`

Rixhon, X., Limpens, G., Coppitters, D., Jeanmart, H.,& Contino, F.(2022). "*The role of electrofuels under uncertainties for the Belgian energy transition.*" In Energies (Vol. 14). URL: `https://doi.org/10.3390/en14134027`

Rixhon, X., Tonelli, D., Colla, M., Verleysen, K., Limpens, G., Jeanmart, H. ,& Contino, F.(2022). "*Integration of non-energy among the end-use demands of bottom-up whole-energy system models.*" In Frontiers in Energy Research, Sec. Process and Energy Systems Engineering, (Vol. 10). URL: `https://doi.org/10.3389/fenrg.2022.904777`

Rixhon, X., Colla, M., Tonelli, D., Verleysen, K., Limpens, G., Jeanmart, H., & Contino, F.(2021). "*Comprehensive integration of the non-energy demand within a whole-energy system: Towards a defossilisation of the chemical industry in Belgium.*" In proceedings of ECOS 2021 conference (Vol. 34, p. 154).

Rixhon, X., Limpens, G., Contino, F., & Jeanmart, H. (2021). "*Taxonomy of the fuels in a whole-energy system.*" In Frontiers in Energy Research, Sec. Sustainable Energy Systems, (Vol. 9). URL: `https://doi.org/10.3389/fenrg.2021.660073`

Limpens, G., Coppitters, D., **Rixhon, X.**, Contino, F., & Jeanmart, H. (2020). "*The impact of uncertainties on the Belgian energy system: application of the Polynomial Chaos Expansion to the EnergyScope model.*" In proceedings of ECOS 2020 conference (Vol. 33, p. 711).

Introduction

It has been proven that the climate change (among other environmental challenges) is (mostly) due to the concentration of anthropogenic greenhouse gases (GHG) in the environment [1]. This concentration resulting from the cumulative emissions (and subtractions), usually expressed in $kt_{CO_2,eq}$, over time could be developed as an adapted, i.e. less economy-oriented, version of the original Kaya identity [2]:

$$\text{GHG} = \frac{\text{GHG}}{\text{Primary energy}} \times \frac{\text{Primary energy}}{\text{EUD}} \times \frac{\text{EUD}}{\text{Population}} \times \text{Population} \quad (1)$$

where the first term represents the global warming potential (GWP) of the primary energy mix, the second is the inverse of the efficiency and the third could stand as the energy intensity per capita. Such an identity, mathematically-correct though, is criticized for the arbitrary choice of variables, the non-independence of them usually leading to the rebound effect and its global/encompassing approach that does not translate properly the heterogeneity of the situation [3]. However, Eq. 1 has the merit to highlight three levers of action that should be activated to reduce the GHG emissions and, consequently, favour the transition. Besides the question of the total population and its growth [4, 5], these three levers of actions are: renewables, efficiency and sufficiency aiming at reducing the first, the second and the third terms on the right-hand side of Eq. 1, respectively. The latter, explicitly mentioned by the IPCC for the first time in 2022 [6], is defined by Lage et al. [7] as "a strategy for reducing, in absolute terms, the consumption and production of end-use products and services through changes in social practices in order to comply with environmental sustainability while ensuring an adequate social foundation for all people". Altough this finds a growing interest in the scientific community [8], it requires, maybe more than the two other levers, interdisciplinarity [9], i.e. the combination of multiple academic disciplines like sociology, psychology or politics, that are out of the scope of my expertise, and, consequently, this thesis. However, the work developed in the present manuscript aims at providing

support to such interdisciplinary projects to assess sufficiency policies. More within the grasp of the engineering world, this thesis rather focuses on the first two terms of Eq. 1, i.e. renewables and efficiency. This aligns with the current European policies binding the Member States of the European Union. For instance, the Renewable Energy Directive (RED) III, published in October 2023 [10], highlights that "the Union's climate neutrality objective (by 2050) requires a just energy transition which leaves no territory or citizen behind, an **increase in energy efficiency** and significantly **higher shares of energy from renewable sources** in an integrated energy system" (i.e. 42.5% of the Union's gross final consumption of energy by 2030).

Consequently, to ensure the energy supply of an assumably more and more demanding society in a context of environmental crisis, major transformations are needed (see Figure 1). Besides behavioral changes, an overall reshape of the energy system is necessary in terms of both primary energy sources, i.e. more renewables, and technologies used to convert these resources into the end-use demand (EUD) (i.e. the energy service required by the the final consumer), i.e. more efficiency [11]. The former corresponds to a whole "fuel switch" (see Figure 1) where energy carriers called, in the literature, "*biofuels*", "*electrofuels*", "*synthetic fuels*", "*renewable fuels*" or even "*sustainable fuels*", will more and more play a crucial role. To avoid the confusion between these fuels and thereby reduce misunderstanding in political or academic discussions, we have suggested a comprehensive and harmonised taxonomy (see Appendix **??**). In the rest of this thesis, the electro - and bio - fuels are considered as renewable and with no GWP.

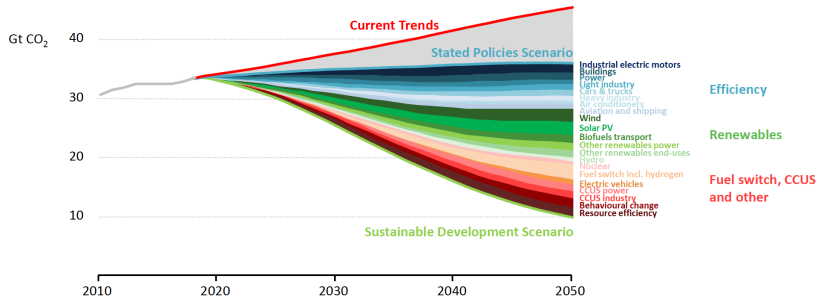

Figure 1. Energy-related CO2 emissions and reductions by sources in the Sustainable Development Scenario [11].

In the general perspective to decrease the GWP of the primary energy mix, variable renewable energy sources (VRES) like wind and solar, have already emerged as the keystone to defossilise the energy system. However, their intermittency and space

disparity could hold back their vaster integration in the future. To address this issue, due to some limitations (e.g. range, power, costs) of electricity-focused solutions like direct current (DC) lines, the transport and long-term storage of the renewable electricity produced in excess should be optimised.

This challenge can be tackled by *electrofuels* [12]. These fuels represent energy carriers where electricity has the major share in the energy balance of the fuel. In practice, this electricity is mainly converted into hydrogen (i.e. electrolysis) and then potentially upgraded into more complex fuels (e.g. methane, methanol or ammonia). Even if the share of electricity increases in the energy system through the electrification of the end-use demand, gaseous and liquid fuels will keep on being big players during (and after) the energy transition [13]. They offer three main advantages: infrastructure compatibility, storage and capacity to link sectors (i.e. from electricity to mobility, heat, or industry). Development on electrofuels aims at getting them more and more compatible with existing and mature technologies [13]. An example is carbon-free ammonia-hydrogen blends burned in spark ignition engines [14] or combined heat and power (CHP) applications [15]. With a growing share of VRES, sector coupling is essential to absorb the surplus of electricity from these intermittent production means [16] and integrate them more cost-effectively [17, 18]. Besides direct electrification of other sectors (e.g. electrical heat pumps, battery electric vehicles), Brown et al. [19] showed that converting power to hydrogen and methane was advantageous at high shares of renewables, in their optimisation of the European whole-energy system. Electrofuels have the ability to couple energy and non-energy sectors [20]. For instance, electricity produced in excess from VRES can be converted in ammonia through the Haber-Bosch process and subsequently transformed into fertiliser - coupling the power and industry sectors [21]. Gas networks present much more storage potential than electrical network (e.g. 50 times more in Germany and 300 times more in France) [22]. Where batteries exhibit limited storage capacity (up to 10 MWh) as well as self-discharge losses, electrofuels are an economical solution for high capacity (from 100 GWh) and long-term (i.e. from months to years) storage of energy [23, 24] (see Figure 2.) Besides storing energy, in their analysis of the German transport sector in 2050, Millinger et al. [25] highlighted that producing electrofuels can represent a better usage of the ambient CO_2 than carbon capture and storage (CCS) to supply hydrocarbon fuels while limiting the curtailment of VRES. Moreover, some applications (e.g. marine, aviation and heavy-duty transport) will be hard to electrify and keep on requiring high-density energy carriers [26, 27]. These carriers, currently produced mostly from fossil resources, will still consist of hydrocarbons in a renewable world. This is why this paper rather uses

"defossilisation" rather than "decarbonisation" as carbon will still play a key role in a carbon-neutral energy transition [28].

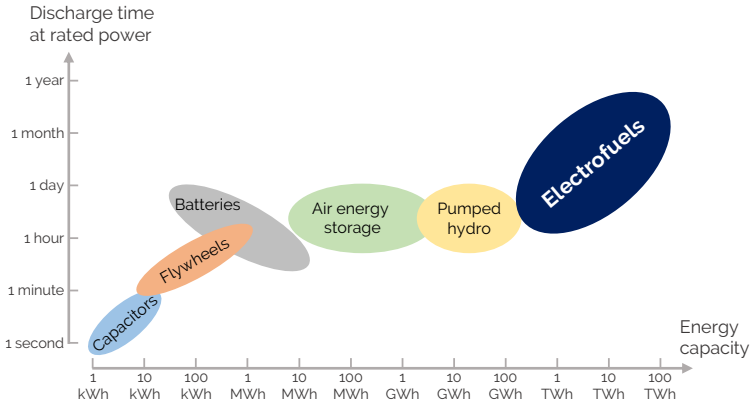

Figure 2. Energy carriers and technologies to store electricity. Electrofuels are an economical solution for high capacity and long-term storage of energy. Graph adapted from [29].

To harvest the maximum potential of synthetic energy carriers in a sustainable transition and maximise the overall system efficiency [30], it is necessary to study the integration of these fuels within a multi-sector and whole-energy system [**?**]. To reach this goal, an energy system optimisation model (ESOM) can define the design of the system to minimise, for instance, its costs or its emissions [31]. In this research field, Yue et al. [32] highlighted that most of ESOMs use a deterministic approach (i.e. 75% out of the 134 reviewed ESOM studies). However, the model structures are inherently uncertain as well as their numerous composing parameters, especially when it comes to define an energy transition strategy for a large-scale system, such as a country. Given the lifetime of the conversion technologies, such strategy implies decisions with long-term impacts (20 to 50 years) where forecasts can be highly unreliable [33]. Besides the uncertainty on the model structure (not addressed in this work), this long-term and large-system optimisation motivates the need to account for Uncertainty Quantification (UQ) and consider it as a major challenge of such models [34]. This challenge, along with a large number (i.e. more than a hundred) of uncertain parameters and limited information of their distribution, leads to the "curse of dimensionality" [35].

It aims at providing decision-makers with new methods and informed policies accounting for the intrinsic uncertainties of the future.

In their 2030 Agenda, United Nations have worked on identifying 17 Sustainable Development Goals (SDGs) as a plan of action for society (or people), environment (or planet) and economy (or prosperity) [36].

From this need, develop a thread like I did in my FRIA application, we need whole-energy system model to give more insights to policymakers

Listing some examples of situations where uncertainties have not been considered and ended up in over-cost/waste of time/waste of..., highlight the need as well to consider uncertainties when we want to advise policymakers.

As the question of policymakers is not only what to do but how to do it, we need to address the optimisation of policies. This would introduce the RL part

In a more sustainable future, some of the energy carriers, currently produced mostly from fossil resources, will still consist of hydrocarbons (e.g. e-methane or e-methanol). This is why this paper rather uses “defossilisation" rather than “decarbonisation" as carbon will still play a key role in a carbon-neutral energy transition [28].

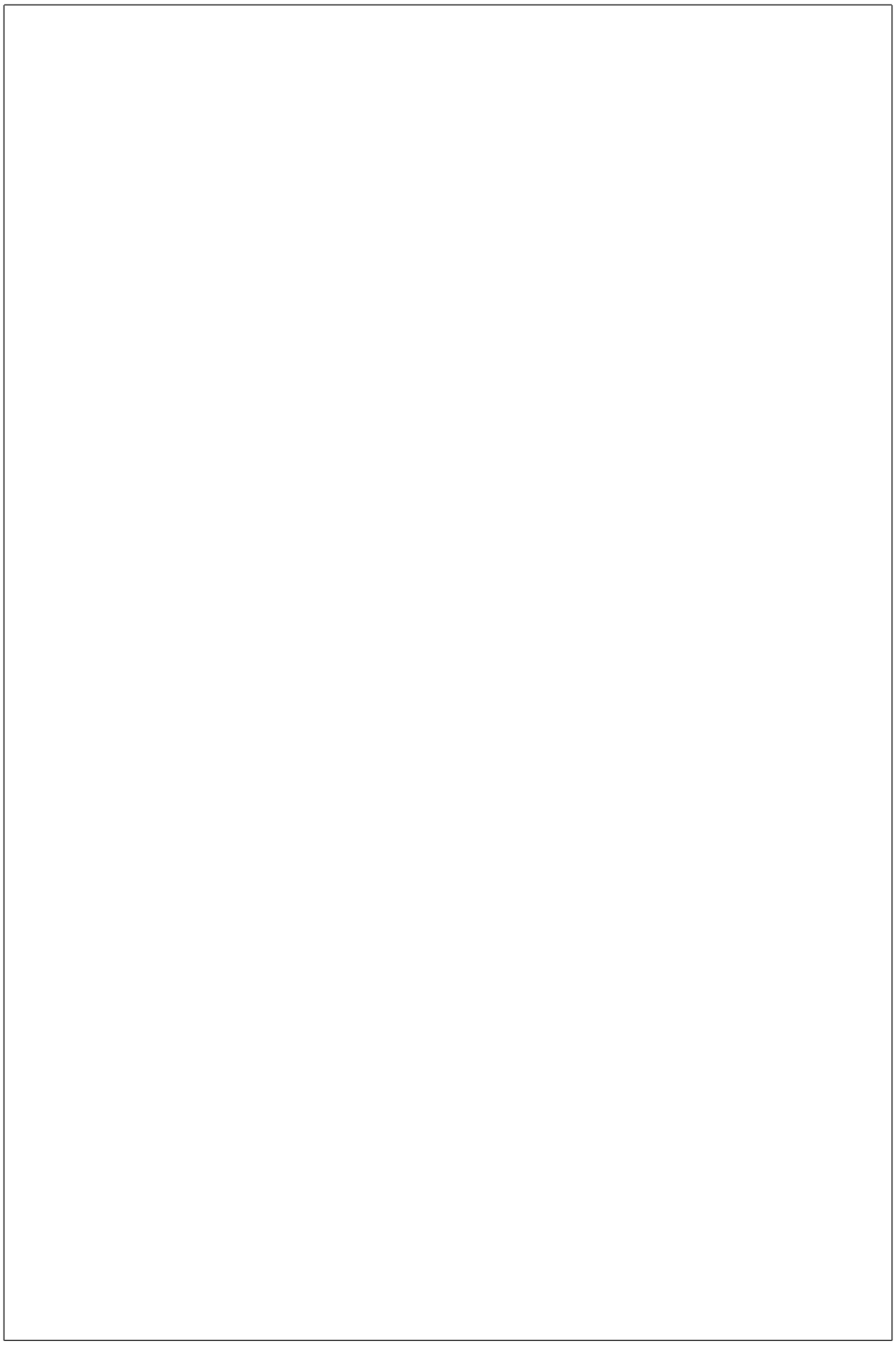

Chapter 1

Methodology: Through a variety of complementary tools

Assessing the robustness of a whole-energy system transition pathway calls a variety of methodological tools. First and foremost, such an extensive system needs to be represented, i.e. modelled, to further be optimized. This model requires some characteristics to capture the peculiarities of this system (e.g. intermittency of VRES, sector coupling) while keeping an affordable computational time and an open-documentation. Then, as looking into the future (i.e. up to 2050 in this work) comes with its lot of uncertainties, these have to be assessed carefully in terms of characterisation and quantification. The former aims at defining the range over which parameters of the model vary. The latter allows assessing the impact that such uncertainties can have on the output of the model. Finally, meeting the environmental objectives while minimizing the cost of the system, accounting for this decision-making process, the uncertainties, and potential shocks/crisis, require therefore a framework to assess the relevance and the timing of the decisions throughout the transition. Finally, given the limited foresight in the uncertain future that has to deal with long-term objective, i.e. limiting the cumulative GHG emissions to a certain budget by 2050, this work encompasses the optimisation of the policy,i.e. set of actions to take along the transition with a specific methodology to assess its robustness.

Detailing the different tools needed to answer the research questions, this chapter starts with the presentation of the whole-energy system optimization model, EnergyScope Pathway and its myopic formulation. Then, the focus is put on the uncertainties, their characterisation as well as quantification. Finally, an agent-based reinforcement learning (RL) approach is detailed to address the sequential decision-making

process in the uncertain transition with limited vision in the future. The robustness of these policies is assessed via the use of the Principal Component Analysis (PCA).

Contributions

The main methodological contribution of this work is the implementation of the reinforcement learning (RL) approach to simulate and optimize the behaviour of an artificial agent interacting with its environment, i.e. the transition of the energy system. Given the uncertainties and potential shocks of the future, this approach allows the agent to play the transition in a sequential, i.e. myopic, way and optimize the choice and the timing of its actions. This optimization is done through multiple tries-and-errors where the agent repeats the transition with a new set of uncertainties.

Then, to support this step-by-step transition with limited foresight in the future, we have extended the EnergyScope Pathway model [37]. Originally developed to optimize the transition in one global optimisation up to 2050, i.e. perfect foresight, part of this thesis consisted in making this model able to optimize the same transition but with sequential more limited time windows, i.e. myopic approach.

The third principal methodological added-value is the use of Principal Component Analysis (PCA) to assess the robustness of a policy. Given the uncertainties and the timespan of the transition, this approach allows highlighting the main "directions" of variation of the system design (i.e. the installed capacities). After this step of identification, strategies and policies can be projected on these directions to see how robust they are to the overall transition uncertainties.

Finally, more minor methodological developments are part of this thesis. Following an approach similar to Guevara et al. [38], we have extended the ranges of uncertainty developed by Moret et al. [33] to the pathway optimisation. After assessing the relevance of using Polynomial Chaos Expansion (PCE) on the optimisation of a whole-energy system [39], we have applied this uncertainty quantification method on the snapshot model subject to different emission-constraints Rixhon et al. [40] as well as the pathway model. Eventually, starting from the initial investigation of Goffaux [41], this work has converged to the most relevant formulation of the salvage value, i.e. $\mathbf{C_{inv,return}}$ in Eq. 1.5, for the model EnergyScope.

Other authors' main contribution statement

Novelty does not stand in the reinvention of the wheel. This thesis, instead, finds its fundamentals in great tools previously developed by other authors. As develop-

ers of the building blocks of the main contributions of this thesis, three main authors are to be mentioned for having brought a significant part of the methodological work. Based on Stefano Moret's monthly whole-energy system model (i.e. EnergyScope) [42], Gauthier Limpens has developed the hourly version of the snapshot model (i.e. EnergyScope TD) [43], as well as the perfect foresight pathway model [44], to which I personally contributed too. Diederik Coppitters has developed the RHEIA framework allowing to quantify the impact of uncertainties and carry out robust optimisation of energy systems [45]. The current work used this framework for the first of these functionalities. Finally, Stefano Moret extensively assessed the uncertainty characterisation on the Swiss energy system [33]. This thesis follows the same methodology, updating the uncertainty ranges for the pathway model.

1.1 Whole-energy system transition model optimisation: EnergyScope Pathway

This work optimises the entire transition pathway from a known system in 2020 up to 2050 thanks to EnergyScope Pathway [44]. According to pathway models review (see Appendix **??**), EnergyScope Pathway can be categorised as an investment and operation optimisation model that assesses the whole-energy system, has a hourly time-resolution and is an open-source documented model. Moreover, it maintains a low computational cost (i.e. around 15 minutes for a 30-year pathway with a hourly discretisation). From the perfect to the myopic foresight of the transition optimisation, this section presents only the main constraints of the former approach to further dig into more details about the latter. The reader is invited to refer to Appendix **??** for more details about the formulation of the model and its extension from a snapshot approach, EnergyScope TD. More extensive information about the formulation choices, for instance, can be found in [44] and the documentation [46].

1.1.1 Perfect foresight: One global optimisation of the transition

The whole-energy system model developed in this work originates from the perfect foresight (PF) formulation (Figure 1.1) of EnergyScope—the entire transition is computed in one optimisation, assuming a complete but uncertain knowledge of the different parameters until 2050 [44]. All the variables and constraints of the snapshot model, EnergyScope TD [43], and summarized in Appendix **??**, are kept as is with an extra-dimension to relate them to a specific representative year, y, of the pathway. For instance, the energy balance is guaranteed at every hour of each of these years.

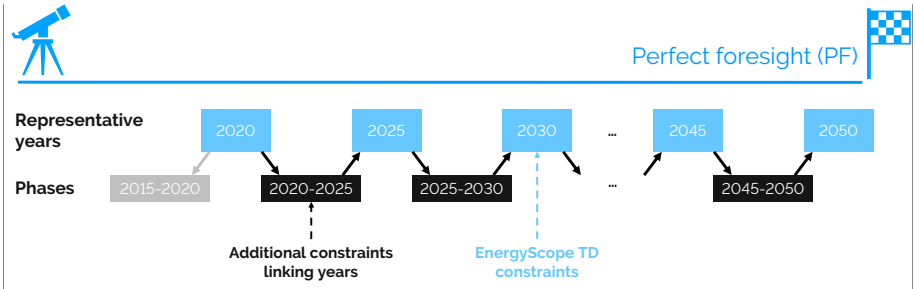

Figure 1.1. Illustration of the pathway methodology based on an existing energy system model. The methodology spans from 2020 to 2050, with one representative year every five years. The model EnergyScope Typical Days (EnergyScope TD) is applied in 7 representative years (light blue boxes). The formulation includes additional constraints (black boxes) that link the years together. The pathway's initialisation assumes that all capacities installed in 2020 were built during the pseudo-phase of 2015-2020 (grey box). The overall problem is defined as the pathway model.

The optimised objective of the pathway model, i.e. the total transition cost $\mathbf{C_{tot,trans}}$, is computed as follows:

$$\min \ \mathbf{C_{tot,trans}} = \mathbf{C_{tot,capex}} + \mathbf{C_{tot,opex}} \tag{1.1}$$

$$\mathbf{C_{tot,capex}} = \sum_{p \in PHASE \cup \{2015\_2020\}} \mathbf{C_{inv,phase}}(p) - \sum_{j \in TECH} \mathbf{C_{inv,return}}(j) \tag{1.2}$$

$$\mathbf{C_{tot,opex}} = \mathbf{C_{opex}}(2020) + t_{phase} \cdot \tau_{phase}(p) \cdot \sum_{p \in PHASE | y_{start} \in P\_START(p), y_{stop} \in P\_STOP(p)} \left(\mathbf{C_{opex}}(y_{start}) + \mathbf{C_{opex}}(y_{stop}) \right) / 2 \tag{1.3}$$

$$\tau_{phase}(p) = 1/(1 + i_{rate})^{diff\_2015\_year(p)} \tag{1.4}$$

$$\mathbf{C_{inv,return}}(i) = \sum_{p \in PHASE \cup \{2015\_2020\} | y_{start} \in Y\_START(p), y_{stop} \in Y\_STOP(p)} \tau_{phase}(p) \cdot \left(c_{inv}(y_{start}, i) + c_{inv}(y_{stop}, i) \right) / 2 \cdot \frac{remaining\_years(i,p)}{lifetime(y_{start}, i)} \left(\mathbf{F_{new}}(p,i) - \sum_{p2 \in PHASE} \mathbf{F_{decom}}(p2,p,i) \right) \quad \forall i \in TECH \tag{1.5}$$

where $t_{phase} = 5$ years and *diff_2015_year(p)* are respectively the duration of a phase between two representative years and the number of years between the middle of a phase and 2015 for a correct annualisation. $\mathbf{C_{inv,return}}$ accounts for the residual value, also called *salvage value*, of the technologies installed during the transition and having

not reached the end of their lifetime by 2050. This last variable is crucial to avoid penalising heavy (and potentially long-lifetime) investments at the end of the transition as these assets would still be operational beyond 2050. The interested reader will find more information about the formulation choices related to it in the work of Limpens et al. [44]. The other variables in Eq. (1.2-1.3) are detailed here below:

$$\mathbf{C_{opex}}(y) = \sum_{j \in TECH} \mathbf{C_{maint}}(y,j) + \sum_{i \in RES} \mathbf{C_{op}}(y,i) \qquad \forall y \in YEARS \tag{1.6}$$

$$\mathbf{C_{inv,phase}}(p) = \sum_{j \in TECH} \mathbf{F_{new}}(p,j) \cdot \tau_{phase}(p) \cdot \left(c_{inv}(y_{start},j) + c_{inv}(y_{stop},j)\right)/2$$
$$\forall p \in PHASE | y_{\text{start}} \in P\_START(p), y_{\text{stop}} \in P\_STOP(p) \tag{1.7}$$

where $\mathbf{F_{new}}$ are the capacities newly installed. In Eq. (1.6-1.7), the costs related to each representative year are:

$$\mathbf{C_{inv}}(y,j) = c_{inv}(y,j)\mathbf{F}(y,j) \qquad \forall y \in YEARS, \forall j \in TECH \tag{1.8}$$

$$\mathbf{C_{maint}}(y,j) = c_{maint}(y,j)\mathbf{F}(y,j) \qquad \forall y \in YEARS, \forall j \in TECH \tag{1.9}$$

$$\mathbf{C_{op}}(y,i) = \sum_{t \in T} c_{op}(y,i)\mathbf{F_t}(y,i,t)t_{op}(t) \qquad \forall y \in YEARS, \forall i \in RES \tag{1.10}$$

where the variable $\mathbf{F}$ represents the size of the installed capacities (for all technologies j) and the variable $\mathbf{F_t}$ is the hourly consumption of the resources; the parameters c_{inv} and c_{maint} are the CAPEX and the OPEX of the technologies, and the parameter c_{op} is the cost of purchasing resources. For the sake of simplicity, as done by Limpens et al. [44], the sum over the 8760 hours of the year is written as the sum over $t \in T$.

Then, as detailed in section **??**, the CO_2-budget for the transition, $\mathbf{GWP_{tot,trans}}$, is computed and constrained as follows:

$$\mathbf{GWP_{tot,trans}} = \mathbf{GWP_{tot}}(2020) + t_{phase} \sum_{p \in PHASE | y_{\text{start}} \in Y\_START(p), y_{\text{stop}} \in Y\_STOP(p)} \left(\mathbf{GWP_{tot}}(y_{\text{start}}) + \mathbf{GWP_{tot}}(y_{\text{stop}})\right)/2 \tag{1.11}$$

$$\mathbf{GWP_{tot,trans}} \leq gwp_{lim,trans} \tag{1.12}$$

where the computation of the yearly emissions are based on the global warming potential (GWP) of the resources:

$$\mathbf{GWP_{tot}}(y) = \sum_{i \in RES} \mathbf{GWP_{op}}(y,i) \qquad \forall y \in YEARS \tag{1.13}$$

$$\mathbf{GWP_{op}}(y,i) = \sum_{t \in T} gwp_{op}(y,i)\mathbf{F_t}(y,i,t)t_{op}(t) \qquad \forall y \in YEARS, \forall i \in RES \quad (1.14)$$

where gwp_{op} is the specific emissions (i.e. in $kt_{CO_2,eq}$/GWh) of each resource. Based on an approach developed by the Intergovernmental Panel on Climate Change (IPCC) [47], this work considers the indicator "GWP100a - IPCC2013" to compute the emissions related to the use of resources. This includes the emissions due to the extraction, the transportation and the combustion of the energy carrier. EnergyScope proposes to account for the embodied emissions of the technologies based on a life cycle assessment (LCA). These stand for extraction of materials, refining, construction and end of life [48]. However, this work is still in progress and the database is not yet complete. Consequently, it is not included in this work and not accounted for.

Besides this constraint on the emissions, the main constraint to link years with each other is the one dictating the installed capacities at the end of each year:

$$\mathbf{F}(y_{\text{stop}}, j) = \mathbf{F}(y_{\text{start}}, j) + \mathbf{F_{new}}(p,j) - \mathbf{F_{old}}(p,j) - \sum_{p2 \in PHASE \cup \{2015\_2020\}} \mathbf{F_{decom}}(p,p2,j)$$
$$\forall p \in PHASE, y_{stop} \in Y\_STOP(p), y_{start} \in Y\_START(p), j \in TECH \quad (1.15)$$

where the variables $\mathbf{F_{old}}$ and $\mathbf{F_{decom}}$ are the capacities respectively having reached the end of their lifetime and prematurely decommissioned. Moreover, to account for the society inertia and to prevent unrealistically fast modal share change, constraints limit this change for the sectors of the low-temperature, the passenger mobility and freight mobility demands. The parameters $\Delta_{\text{change,LT\_heat}}$, $\Delta_{\text{change,pass}}$ and $\Delta_{\text{change,freight}}$ respectively limit their respective modal share change up to 33%, 50% and 50% per phase of 5 years.

1.1.2 Myopic: Sequential optimisation of the transition with limited foresight

One of the main methodological contributions of this work regarding the development of the whole-energy system model consists in giving it the possibility to optimise the transition pathway in a myopic approach.After introducing the general concept of it, this section details more the additions brought to the model in terms of implementation.

General concept of the myopic optimisation

Compared to the perfect foresight, the myopic approach (Figure 1.2) has two main advantages: shorter computational time and more realistic representation of the shortsightedness of decision-makers. For this reason, several studies are based on this ap-

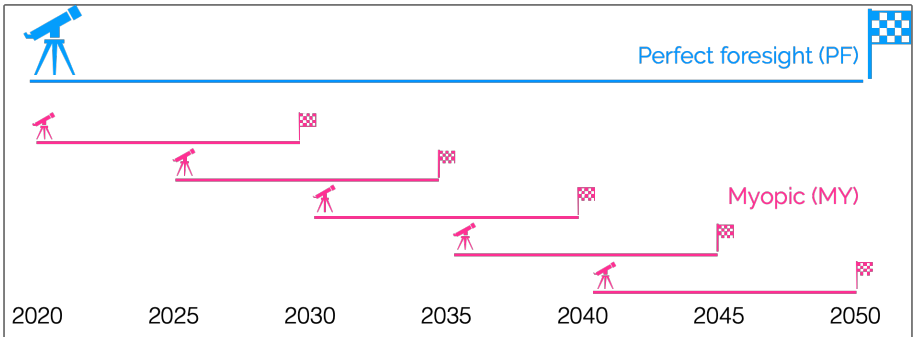

Figure 1.2. The myopic approach (in pink) uses several instances of the pathway model (illustrated in Figure **??**). In this example, the pathway instance has a time horizon of 10 years ($N_{\text{year,opti}} = 10$) with a 5 year-overlap ($N_{\text{year,overlap}} = 5$). As a comparison the Perfect foresight (in blue) has a time horizon of 30 years.

proach [49–52]. Babrowski et al. [49] analysed the benefit of the myopic approach to reduce the computational time. Poncelet et al. [50] uses this approach to analyse the expansion planning of the power sector beyond 2050. Nerini et al. [51] analysed the impact of the horizon windows and overlapping time. Overall these studies decided to choose the myopic approach to analyse the speed of change compared to a perfect foresight approach. Moreover, the myopic approach allows a sequential optimisation process that opens the doors to decision-making/policy-learning methodologies, like assessing shock events. This approach is used by Heuberger et al. [52] who assessed the speed of integration of technologies due to these events. In their analysis of the overcapacity in European power systems, Moret et al. [53] emphasised that such a "possibility of *recourse*" is very appropriate to address uncertainty gradually unfolding over time. Consequently, the development of the myopic approach represents the foundations of the further implementation of the agent-based reinforcement learning framework (see Section 1.3).

As illustrated in Figure 1.3, after optimising, in design and operation, one time window (e.g. from 2020 to 2030), the intermediate system design (i.e. the installed capacities) is set as initial conditions for the start of the next time window (e.g. from 2025 to 2035) as well as the historical investment decisions (i.e. $\mathbf{F_{new}}$, $\mathbf{F_{old}}$ and $\mathbf{F_{decom}}$). Consequently, the solution obtained at the end of the first time window (e.g. 2030) as well as potential investment decisions between the start of the second time window and this end-year are discarded. In other words, they are not taken into account for the optimisation of the second time window. This process goes on until the stated end of the transition (i.e. 2050, in this case).

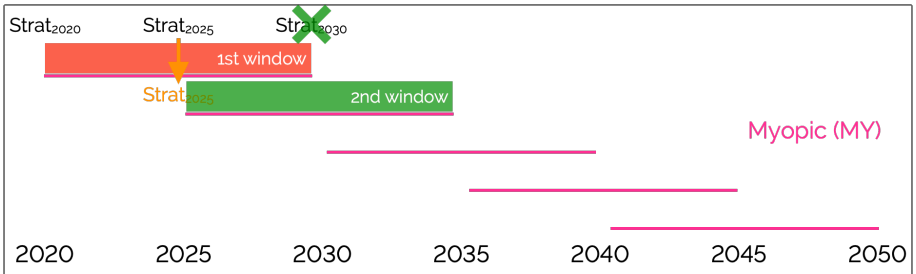

Figure 1.3. Sequential optimisation of the transition pathway in the myopic approach: (i) first time-window optimisation, (ii) set-up of the initial conditions of the second time-window, (iii) second time-window optimisation discarding intermediate results

Additional sets, parameters and variables

The major add-on from the original EnergyScope Pathway model [37] to the myopic version developed in this thesis, is the possibility to carry out the optimisation on a limited time window, of which the duration is defined by $N_{\text{year,opti}}$. Moreover, to ensure the "possibility of *recourse*", there is also the possibility of having an overlap between two consecutive time windows. The timespan of this overlap is defined by the parameter $N_{\text{year,overlap}}$. The philosophy followed behind the development of the myopic approach was to add another layer on top of the perfect foresight model in order to make it more modular. For this reason, the already existing constraints are marginally adapted. This way, the newly developed model can easily be used to perform a perfect foresight optimisation by setting the time window to $N_{\text{year,opti}}$ =30 years (i.e. between 2020 and 2050) and the overlap between the time windows to $N_{\text{year,overlap}}$ =0. Consequently, as defining the actual time window on which the system is optimised as well as the history, i.e. what has already been optimised earlier in the transition, are fundamental, four new sets are implemented: $\text{YEARS}_{\text{WND}}$, $\text{YEARS}_{\text{UP TO}}$, $\text{PHASE}_{\text{WND}}$ and $\text{PHASE}_{\text{UP TO}}$ (see Table 1.1).

$\text{YEARS}_{\text{WND}}$ and $\text{PHASE}_{\text{WND}}$ substitute YEARS and $textPHASE$ in the constraints defined in the pathway model in Section 1.1.1. These two sets aim at setting the optimization to a more limited time window. Progressing through the transition, $\text{YEARS}_{\text{UP TO}}$ and $\text{PHASE}_{\text{UP TO}}$ allow keeping track of the history of the investments (e.g. technologies installation, decommissioning or retirement), the consumption of resources, the cumulative amount of emissions, etc.

On top of these four specific sets, some artefacts were also necessary to avoid computational rounding errors. Indeed, optimizing the first year of a time window that has already been optimized in the previous time window could lead to rounding errors

Table 1.1. New SETs for myopic pathway formulation.

Set	Index	Description
$\text{YEARS}_{\text{WND}}$	$y \in \text{Y}$	Representative years of the time window to optimize
$\text{YEARS}_{\text{UP TO}}$	$y \in \text{Y}$	Representative years including the years already optimised, i.e. the history
$\text{PHASE}_{\text{WND}}$	$p \in \text{P}$	Phases of the time window to optimize
$\text{PHASE}_{\text{UP TO}}$	$p \in \text{P}$	Phases including the phases already optimised, i.e. the history

preventing from the optimization to converge. For this reason, the set YEAR_{ONE} accounts for the first representative year of the time window to optimize that is excluded from $\text{YEARS}_{\text{WND}}$ to avoid these errors. This remark stays valid for any time window except the first one of the transition where the year 2020 is optimized even though its technological strategy is set according to the actual system presented in Appendix **??**. Finally, as the end of time windows changes for each of them, the parameter *remaining_years* has to be updated accordingly to keep a meaningful definition of $\mathbf{C_{inv,return}}$ in Eq. 1.5.

Myopic pathway implementation

Starting this work in 2017, AMPL Optimization Inc. has developed a Python application programming interface (API) called amplpy [54]. In a nutshell, this API allows the pre/post-processing of an ampl optimisation problem by accessing its features (e.g. constraints,parameters, variables, objective function) from within Python. Using thisAPI, this updated version of the model interacts with the AMPL problem representing the optimization of the whole-energy system transition pathway as represented in Figure 1.4.

Impact of myopic formulation on the system

As expected, the computational time is reduced drastically (i.e. by 55%) while the design remains similar. Given the continuous change of the input parameters over the considered time frame, the perfect foresight and myopic approaches results are very similar, like in [55]: less than 1% cost difference over the transition, similar system designs by 2050 and slight shifts in time in terms of adoption of technologies.

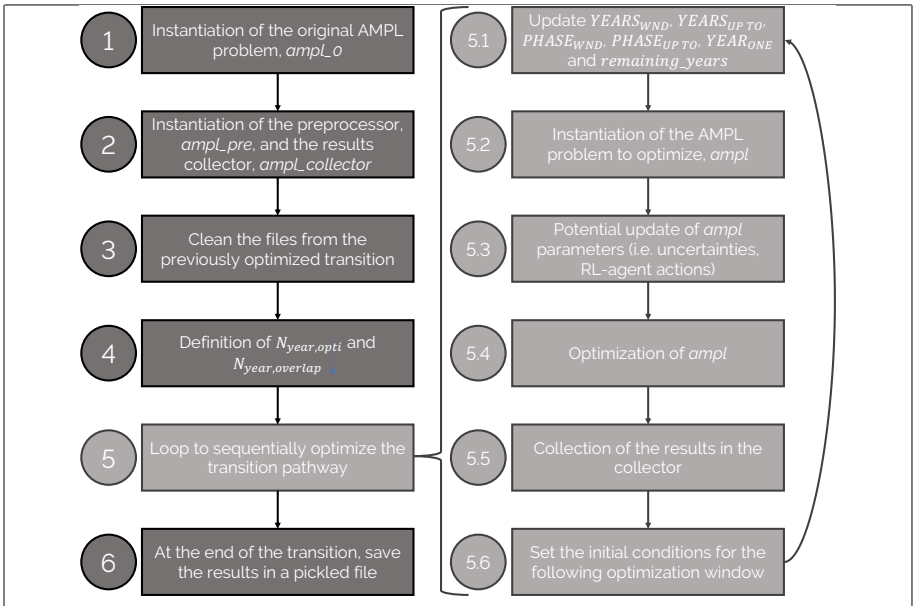

Figure 1.4. Schematic of the iterative optimization of the whole-energy system transition pathway.

The main difference lies in the transition itself and especially in the earlier deployment of PVs and offshore wind turbines. These induce the reinforcement of the grid that is a capital-intensive and long-lifetime asset. This is mostly due to the chosen formulation of the salvage value, Eq. 1.5. Since the objective function is now the transition cost over a more limited time window (i.e. 10 years rather than 30 years), a bigger salvage value, deduced from the total investments, leads to a temporary better optimum at early stages of the transition. A more detailed comparison between the myopic and perfect foresight approaches is available in Appendix **??**.

1.2 Uncertainty quantification

In their systematic review, Yue et al. [32] highlighted that a wide majority of studies addressing the optimisation of energy systems (i.e. 75% out of the 134 reviewed studies) were not investigating the impact of uncertainties. However, disregarding these impacts can have drastic consequences on the system design. For instance, historical low fossil gas (NG) prices have led to overcapacity of combined cycle gas turbine (CCGT) in Europe [53]. This is why accounting for uncertainty in energy system optimisation

models (ESOMs) is crucial [56], especially when it comes to optimise several decades in an inherently uncertain future [57].

This section aims at briefly presenting the methods followed to first characterise these uncertainties, then to quantify their impact on different outputs of interest of the model (e.g. amount of molecules imported from abroad, the installed capacity of small modular reactor (SMR) or the total transition cost) and finally, the screening and selection of the parameters to analyse.

1.2.1 Uncertainty characterisation

Characterising precisely the uncertainty—ideally with their respective probability density functions (PDFs)—of the thousands of parameters in the model is daunting if not impossible because of lack of data [58]. Therefore, we used a workaround developed by Moret et al. [33] that defines relative ranges of variation for different groups of parameters. These ranges have been adapted for the Belgian energy system and the pathway formulation. Moreover, some ranges have been added to account for new parameters coming from the pathway formulation described in Section 1.1 like the society inertia. Like other works [59, 60], the uncertain parameters are assumed to be independent and uniformly distributed between their respective lower and upper bounds.

Following the methodology defined by Moret et al. [33], uncertainties of types I (investment-type) and II (operation-type, constant uncertainty over time) keep the same range for the whole transition. However, parameters with an uncertainty increasing over time, type III, (i.e. end-use demands, in this case) will have a wider and wider range over the transition. In this work, a +50% linear increase has been arbitrarily set between the width of the range of such parameters in 2025 and the same ranges in 2050. In Figure 1.5, this means that for type III uncertainties only, R^{+}_{2050} is 50% bigger than R^{+}_{2025} and R^{-}_{2050} is 50% smaller than R^{-}_{2025}. For uncertainties of types I and II, the relative variation versus the nominal value remain the same over the transition. Inspired by Guevara et al. [38], the values of the uncertain parameters are set at a fixed relative position from the nominal values for each sampled transition—the values do not zigzag from 2025 to 2050 within the bounds (Figure 1.5).

Finally, the model accounts for thousands of parameters. The computational burden to consider all of them separately would be completely overwhelming ($\sim 10^7$ model runs). Therefore, similarly to other works [33, 39], the model parameters that would follow the same uncertainty have been grouped to one single uncertain parameter. For instance, the uncertainty on the cost of purchasing renewable electrofuels,

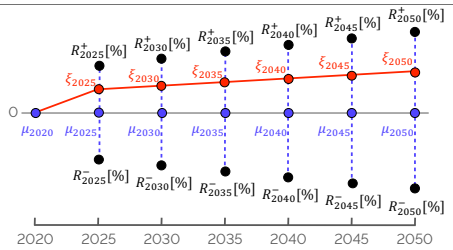

Figure 1.5. μ_{2020}, μ_{2025}, ..., μ_{2050} are the nominal values equal to 0 as the uncertain parameters represent a relative increase/decrease of actual parameters of the model. R^+ and R^- are respectively the upper and lower bounds of the range and ξ_{2025}, ξ_{2030}, ..., ξ_{2050} are the values taken by one parameter for a specific sample of the global sensitivity analysis (GSA) for each of the representative years of the transition, always starting from the nominal value in 2020, μ_{2020}. The graph has been adapted from [38].

$c_{\text{op,electrofuels}}$, identically affects the cost of e-hydrogen, e-methane, e-ammonia and e-methanol. Indeed, besides their respective specificities, each of these fuels will be similarly affected by the variation of cost of electricity or the electrolyser, that drive the majority of their cost of purchasing [61]. Similarly, the uncertainties impacting the industrial demand, $industry\_EUD$, alters equally the industrial high- and low-temperature and electricity demands as well as the non-energy demand.

1.2.2 Polynomial Chaos Expansion

We used Polynomial Chaos Expansion (PCE), an approach for surrogate-assisted UQ, to propagate uncertainties in input parameters through the system model. This allowed us to assess statistical moments on the quantity of interest and determine Sobol' indices [62]. To construct a PCE of the EnergyScope Pathway model, we employed the open-source Python framework RHEIA [63, 64]. Where the first part of this section is dedicated to the mathematical definition of this approach, the second details its choice and summarises the comparison made with another approach (i.e. Morris method) in a previous work [39].

Definition

The PCE model ($\hat{M}$) is a representation of the relationship between the input parameters and the output variable of interest (i.e. results) in the EnergyScope Pathway model (M). This representation is constructed as a truncated series of multivariate orthonormal polynomials $\mathbf{\Psi}$, weighted by coefficients u:

$$\hat{M}(\boldsymbol{\xi}) = \sum_{\boldsymbol{\alpha} \in \mathcal{A}^{d,p}} u_{\boldsymbol{\alpha}} \boldsymbol{\Psi}_{\boldsymbol{\alpha}}(\boldsymbol{\xi}) \approx M(\boldsymbol{\xi}), \tag{1.16}$$

where the vector $\boldsymbol{\xi} = (\xi_1, \xi_2, \dots \xi_d)$ comprises the independent random input parameters (**??**), d corresponds to the number of input distributions and $\boldsymbol{\alpha}$ is a multi-index, i.e. a vector of non-negative indices of length d, where each index corresponds to the degree of each univariate polynomial that forms the basis of the multivariate polynomial $\boldsymbol{\Psi}_{\boldsymbol{\alpha}}$. As uniform distributions are considered, the Legendre polynomials are adopted, as they are the associated family of polynomials that are orthogonal with respect to standard uniform distributions [65].

A truncation scheme is implemented to restrict the number of multivariate polynomials in the series. This is done based on two factors: a specified limiting polynomial order (p) and the number of uncertain parameters (d) involved. The multivariate polynomial order $|\boldsymbol{\alpha}|$ is the summation of the orders for each univariate polynomial in the multivariate polynomials space. Thus, only the multi-indices corresponding to an order that is less than or equal to the specified limiting order are retained and stored in the truncated series denoted as $\mathcal{A}^{d,p}$:

$$\mathcal{A}^{d,p} = \left\{ \boldsymbol{\alpha} \in \mathbb{N}^d \, : \, |\boldsymbol{\alpha}| \leq p \right\}. \tag{1.17}$$

The number of multi-indices satisfying this condition is as the cardinality of $\mathcal{A}$, i.e. the number of its elements:

$$\text{card}\left(\mathcal{A}^{d,p}\right) = \binom{p+d}{p} = \frac{(d+p)!}{d!p!} = P + 1. \tag{1.18}$$

The coefficients $(u_0, u_1, \dots, u_{P+1})$ are quantified using a regression method applied to orthonormal polynomials [65]. To ensure a well-posed least-square minimisation, it is recommended to have a number of training samples at least twice the number of coefficients [65]. Therefore, $2(P+1)$ samples are evaluated in the system model, and the model response for each quantity of interest is recorded. To generate the training samples, the quasi-random Sobol' sampling technique is employed [66]. As a low-discrepancy sequence, this technique exhibits the main advantage to investigate efficiently and (almost) uniformly the hypercube of uncertainties, unlike uniformly distributed random numbers.

The process of defining the polynomial degree includes incrementally increasing it until a desired level of accuracy is achieved [63]. Starting with $p = 1$, a PCE is constructed and the leave-one-out (LOO) error is evaluated. If the LOO error is below a specified threshold, the corresponding polynomial order is considered sufficient for

generating an accurate PCE. However, if the error exceeds the threshold, the order is increased, and additional samples are generated following the rule of Eq. (1.18).

For the specific study of this work, a polynomial order of 2 is necessary (with 1260 training samples as per Eq. (1.18)) to achieve a LOO error below 1 % for the total transition cost.

Lastly, the statistical moments can be analytically derived from the PCE coefficients, eliminating the need for further model evaluations. The mean μ and standard deviation σ are obtained as follows:

$$\mu = u_0, \tag{1.19}$$

$$\sigma^2 = \sum_{i \neq 0} u_i^2. \tag{1.20}$$

Furthermore, the Sobol' indices can also be determined analytically. The total-order Sobol' indices (S_i^T) assess the overall influence of a stochastic input parameter on the performance indicator, encompassing all possible interactions:

$$S_i^T = \sum_{\boldsymbol{\alpha} \in A_i^T} u_{\boldsymbol{\alpha}}^2 / \sum_{i=1}^{P} u_i^2 \qquad A_i^T = \{\boldsymbol{\alpha} \in A | \alpha_i > 0\}. \tag{1.21}$$

Here, A denotes the collection of all PCE coefficients, and α_i corresponds to the coefficient associated with the uncertain parameter i.

Comparison with a proven method

Besides being an in-house used method, an early step of this thesis consisted in assessing PCE with similar approach used in the literature [39].

After characterising the uncertainty ranges, Moret et al. [33] quantified the impact of these uncertainties on the snapshot model of EnergyScope, i.e. ranking them, using the Morris method [67]. This method, as a statistical analysis, relies on individually randomized one-factor-at-a-time designs. Given the d model parameters $\vec{\xi} = (\xi_1, \xi_2, ..., \xi_d)$, the first step of the method consists in generating independent random samples of $\vec{\xi}$ in a standardised and discretised p-level *region of experimentation*, ω. In this *region of experimentation*, each ξ_i, varying in the interval $[\xi_{i,min},\ \xi_{i,max}]$, can take a random discrete value as follows :

$$\xi_i = \xi_{i,min} + j \cdot \frac{1}{p-1} \left(\xi_{i,max} - \xi_{i,min}\right) \quad \text{with } j \in \{0, 1, ..., p-1\} \tag{1.22}$$

Then, given these random one-factor-at-a-time samples, Morris method defines, for a given set of $\vec{\xi}$, the elementary effect of the ith parameter (EE_i) as :

$$EE_i = \frac{M(\xi_1, \xi_2, ..., \xi_i + \Delta, ..., \xi_d) - M(\vec{\xi})}{\Delta} \tag{1.23}$$

where M is the objective function, $\vec{\xi} \in \omega$, except $\xi_i \leq 1 - \Delta$ and Δ is a set multiple of $1/(p-1)\left(\xi_{i,max} - \xi_{i,min}\right)$. As in other studies [33, 68, 69], we consider p as even and $\Delta = p/[2(p-1)]\left(\xi_{i,max} - \xi_{i,min}\right)$.

Finally, in order to evaluate the importance of the ith parameter over an output, Morris method relies on F_i, the distribution of r elementary effects. Computing the mean, $\mu_i = \mu(F_i)$, and the standard deviation, $\sigma_i = \sigma(F_i)$, of the F_i distribution, allows ranking the parameters based on their influence on the concerned output. Usually, in Morris method, p and r respectively get values as follows : $p \in \{4, 6, 8\}$ and $r \in [15; 100]$ depending on, d, the number of uncertain parameters. The higher this number is, the higher shall be, simultaneously, p and r. In the following comparative analysis, we set p and r to their maximum values, respectively 8 and 100 in order to get the most reliable parameters ranking.

Beyond the original Morris method, we used the standardized elementary effects, SEE_i, formulation [68], given by

$$SEE_i = EE_i \cdot \frac{\sigma(\xi_i)}{\sigma(M)}. \tag{1.24}$$

Among other things, the SEE allows comparing the influence of different inputs on the same output or compare the influence of a same parameter on different outputs, even if these parameters or outputs are significantly different in terms of variation range or average amplitude. Moreover, this standardized analysis does not require any additional model evaluations.
Therefore, in the following results, we rather use

$$\mu_i^* = \mu(|SF_i|) \tag{1.25}$$

to rank parameters among each other. In (1.25), SF_i is the distribution formed by the r standardized elementary effects, as done in Moret [69].

In [39], we have assessed the PCE approach, comparing the Top-14 most impacting parameters obtained from this approach with the one provided by the improved Morris method based on μ_i^*. Even if the output of each method does not have the same physical

meaning, both methods can rank the parameters by their impact on the total annual cost of the energy system. Both rankings were very similar which validates the use of PCE in the rest of this work.

1.2.3 Preliminary screening and selection

After the initial phase of grouping (Section 1.2.1), a preliminary screening was necessary to identify the key parameters to account for in this GSA. Rixhon et al. [40] performed a similar sensitivity analysis on the 2050 Belgian whole-energy system under different CO_2-limits using the snapshot model, i.e. EnergyScope TD [43]. Screening the results of this work, we have discarded some parameters with negligible impact (e.g. CAPEX of electrolysers or variation of the freight demand), selected a subset of parameters and added others that were intrinsic to the pathway formulation, e.g. modal share changes, or related to the integration of SMR, $f_{\text{max,SMR}}$. The exhaustive list of these 34 parameters is presented in Appendix **??**.

1.3 Agent-based reinforcement learning for energy transition support

The transition towards carbon-neutrality of a whole-energy system (i.e. including all streams of energy carriers and demands) is uncertain. Therefore, instead of establishing single-shot definitive plans towards 2050 (and beyond), i.e. perfect foresight, policy makers rather go through multiple rolling-horizon short-term decisions, i.e. myopic approach. Yet, these decisions can have long-term impacts, 20 to 50 years. Meeting the environmental objectives while minimizing the cost of the system, accounting for this decision-making process, the uncertainties, and potential shocks/crisis, require therefore a framework to assess the relevance and the timing of the decisions throughout the transition. To navigate through the transition and investigate the efficiency of different policies, this work implements the reinforcement learning approach. This section aims first at presenting the general concepts of this approach as well as the policy optimisation algorithm. Then, the environment, actions, state and reward are detailed.

1.3.1 Reinforcement learning fundamentals and application to energy systems

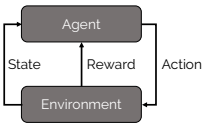

Figure 1.6

RL is a subfield of machine learning focused on training an agent to make sequential decisions by interacting with an environment to achieve specific goals. Unlike supervised learning, where data is labeled, and unsupervised learning, where patterns are inferred from unlabeled data, reinforcement learning deals with learning from interaction, typically through trial and error. This way, RL is considered as active learning [70]. Starting from an initial state, the agent takes an action that impacts its environment. The latter feeds back the agent with a reward and the new state (see Figure 1.6). This goes on until reaching the end of the episode. When the episode is done, the agent starts again from an initial state, takes an action and so on. The agent learns to optimize its policy by maximizing a notion of cumulative reward over time. This policy refers to the strategy or mapping from states to actions that the agent employs to make decisions. Essentially, it defines the behavior of the agent in the environment. The ultimate goal of the agent is often to find an optimal policy, which maximizes the expected cumulative reward over time. All these concepts and interactions between the agent and its environment are formalized as a Markov decision process (MDP) [71], represented by the tuple $< s, a, T, r, \pi, \gamma >$. $s \in S$ is the state defined in a certain state space, S, that represents the observable parts of the environment that the agent uses to make decisions. $a \in A$ is the action among the action space, A, and T is the probability of transitioning from one state s to another state s' given a specific action, a: $T(s, a, s') : \Pr\left(s'|s, a\right)$.$r$ is the reward received by the action when taking the action a from a state s, $R(s, a)$. Finally, π is the policy as already described and γ is the discount factor that controls the importance of future rewards versus immediate rewards. During the learning/optimization process, the agent acts according to the exploitation-exploration trade-off. In the former case, the action a is directly given the mapping provided by the current policy π, depending on the state s. In the latter, the action is randomly picked within the action space. For further information, the interested reader is invited to refer to work of Sutton and Barto [71] or the course given by David Silver [72] available online.

Due to the increasing complexity of the systems and the integration of uncertainties, the last decades have seen the emergence of publications where RL is applied to energy systems [73]. In their respective reviews, Cao et al. [70] and Perera and Kamalaruban [73] highlighted groups of problems addressed with RL in the research field of energy systems: building energy management system (BEMS), optimization of dispatch and operational control closely linked with the energy market and the optimal power flow problem in the grid, micro-grid management, electro-mobility or even demand-side management or optimal control of energy system devices like maximum

power point tracking (MPPT) of wind turbines and photovoltaic (PV) panels. The major novelty of this thesis in the use of RL stands then in its application to a new kind of energy system problem: the optimization of the transition pathway of a whole-energy system. In this sense, the objective is to optimize and provide a policy to support this transition subject to uncertainties.

1.3.2 Problem formulation and algorithm

At the initial state, i.e. the energy system in 2020, the agent gets an initial observation, $\boldsymbol{o}_0$. An observation represents a set of the characteristics of the environment accessible to the agent for it to take the next action. The state, though, is the exhaustive list of these characteristics. Even though an observation is a subset of the state, this work uses these two words interchangeably. Then, it takes an action, $\boldsymbol{a}_0$, impacting its environment, i.e. the energy system limited transition over the first decision window (2020-2030). Through this interaction with its environment, the agent is given a reward, $r_1 = r\left(\boldsymbol{a}_0|\boldsymbol{o}_0\right)$, and ends up in a new state, i.e. the energy system in 2025, characterised by a new observation, $\boldsymbol{o}_1$, and so on (see Figure 1.7).

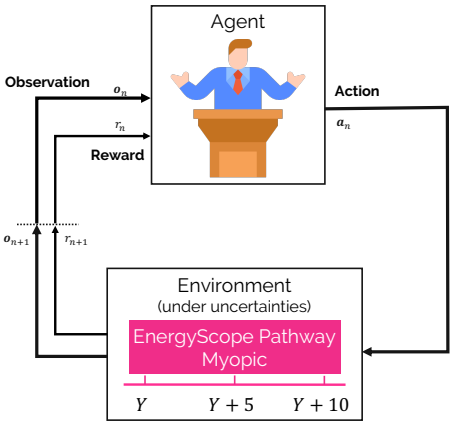

Figure 1.7. Reinforcement learning (RL) framework made of the agent interacting with its environment, i.e. the energy-system model on a limited decision window of 10 years.

A learning episode is a succession of such learning steps. In the context of the transition pathway between 2020 and 2050, an episode can come to an end for different reasons. First, if the actions taken by the agent make the optimisation infeasible, the episode is prematurely stopped before reaching 2050. Similarly, cumulative emissions

of the system over the predefined CO_2-budget (see Section **??**) lead to an anticipated end of the episode. Finally, the "natural" end is the prescribed end of the transition, i.e. 2050. Consequently, the maximum value of steps for an episode is equal to $N_{ep,max} = 5$.

The goal of a RL approach is to optimise the mapping between inputs (i.e. the observations) and output (i.e. the actions), called the policy $\pi\left(\boldsymbol{a}_n|\boldsymbol{o}_n\right)$. To do so, an objective function, $\boldsymbol{J}(\pi)$, built on the cumulative rewards collected during each episode. Finally, a back-propagation process updates the weights and biases of the neural network (NN) during the learning of the agent. Among the wide variety of RL algorithms applied in energy systems [73], this work opted for Soft Actor Critic (SAC) [74] to train and update the NN. This algorithm is model-free and off-policy. The former characteristic is necessary as the agent is assumed to have no knowledge about the dynamics of the environment, i.e. its transition or reward functions. The transition function is, given the current state of the environment and the action taken by the agent, a function that outputs a probability to end up to any of the next states. The reward function, on its turn, gives a reward given the current state and the taken action. In practice, in this model-free approach, the agent estimates the optimal policy directly from experience and without estimating the dynamics of the environment. However, model-free methods suffer from two major drawbacks: their sample inefficiency and their brittleness with respect to their hyper-parameters (e.g. learning rates, exploration constants) [74]. The former leads to a too expensive computational burden while the second requires meticulous settings to get good results. SAC overcomes these two challenges as an off-policy (i.e. efficiently re-using past episodes to update the target policy-network) actor-critic deep RL algorithm based on the entropy-augmented objective function:

$$\boldsymbol{J}(\pi) = \mathop{\mathbb{E}}_{\pi}\left[\sum_{n=0}^{N_{ep}} \gamma^n r_n\left(\boldsymbol{o}_n, \boldsymbol{a}_n\right) - \zeta \log\left(\pi\left(\boldsymbol{a}_n|\boldsymbol{o}_n\right)\right)\right] \tag{1.26}$$

where γ is the discount factor and ζ the temperature parameter. The former determines how much importance we want to give to future rewards within an episode. The latter balances the trade-off between exploitation of proven actions via the return maximisation, i.e. $\sum_{n=0}^{N_{ep}} \gamma^n r_n\left(\boldsymbol{o}_n, \boldsymbol{a}_n\right)$, and exploration through the entropy[1] term, i.e. $\log\left(\pi\left(\boldsymbol{a}_n|\boldsymbol{o}_n\right)\right)$. This way, SAC ensures sample efficiency and low sensitivity to hyper-parameters while improving exploration [75] and robustness [76]. These make SAC a state-of-the-art algorithm and one of the most efficient model-free deep RL

[1] Where entropy represents the amount of energy in a system not available to produce work in thermodynamics, this term stands for the randomness or stochasticity of the policy in the current context.

method nowadays. In this work, the authors used the open-source SAC package developed by STABLE-BASELINES3 [77] where the policy NN is a fully connected multilayer perceptron (MLP) built with TENSORFLOW [78]. For further information on RL and the SAC algorithm, the interested reader is invited to refer to the works of Sutton and Barto [71] and Haarnoja et al. [74], respectively.

1.4 Robustness assessment via PCA

When optimizing a transition pathway of a whole-energy system, including its uncertainties, capturing the most variable changes of design (i.e. installed capacities of each technology) can become overwhelming due to the curse of dimensionality. For the case study detailed in Chapter **??**, this consists of i.e. 7 representative years of the transition (i.e. from 2020 to 2050), 113 possible technologies subject to uncertain parameters. To tackle this challenge, we have developed a methodology based on the Principal Component Analysis (PCA). This methodology provides two main outputs. First and foremost, using the model runs necessary to quantify the impact of the uncertain parameters on the total cost of the transition (see Section 1.2), it gives a metric on which to assess the robustness of energy transition policies resulting from different approaches. This metric gives more insight that, for instance, the variation of the total transition cost that encompasses too many aspects (i.e. design and operation strategies, variation along the transition) in one single value. Second, these "directions of variation" can highlight key modal shifts or highly varying design strategies over the transition. After introducing the general concept of PCA, this section aims at detailing the methodology proposed to give these "directions of variation" and to assess the robustness of policies.

1.4.1 Principal Component Analysis: General concept

Born in the early 20th century [79, 80], the Principal Component Analysis (PCA) finds its fundamentals from the singular value decomposition (SVD). The latter is a generalization, to an arbitrary (i.e. not especially square) matrix, of the spectral theorem stating that a normal matrix can be diagonalized by an orthonormal basis of eigenvectors. The core concept of principal component analysis (PCA) involves simplifying a dataset with numerous interconnected variables by reducing its dimensionality. The aim is to preserve as much variability within the data as feasible. This is accomplished by transforming the data, $\mathbf{x}$, into a new set of variables called principal components (PCs), $\mathbf{z}$. These components are uncorrelated and arranged in such a way that the first

ones retain the majority of the variability found in all of the original variables. On the other hand, the final principal components (PCs) pinpoint directions where there is minimal variation, indicating nearly constant linear relationships among the original variables [81].

Easier to represent in two dimensions, let us consider a vector $\mathbf{x}$ composed of the variables x_1 and x_2, $p = 2$, and 25 realisations of them (See Figure 1.8 (left)). The first principal component (PC), z_1, is a linear function, $\boldsymbol{\alpha}_\mathbf{1}^\mathbf{T}\mathbf{x}$, of the different variables of x with maximum variance:

$$z_1 = \boldsymbol{\alpha}_\mathbf{1}^\mathbf{T}\mathbf{x} = \alpha_{11}x_1 + \alpha_{12}x_2 + ... + \alpha_{1p}x_p = \sum_{j=1}^{p} \alpha_{1j}x_j \tag{1.27}$$

where ^{T} means the transpose vector. Then, $z_2 = \boldsymbol{\alpha}_\mathbf{2}^\mathbf{T}\mathbf{x}$, is another linear function of $\mathbf{x}$,uncorrelated with z_1 and maximizing the variance. These transformations lead to the construction of the PCs (see Figure 1.8 (right)). In more general cases, one can write $z_k = \boldsymbol{\alpha}_\mathbf{k}^\mathbf{T}\mathbf{x}$ as the k^{th} PC. There can be up to p PCs even though, usually, most of the variance of the original data can be captured by m PCs where $m \ll p$.

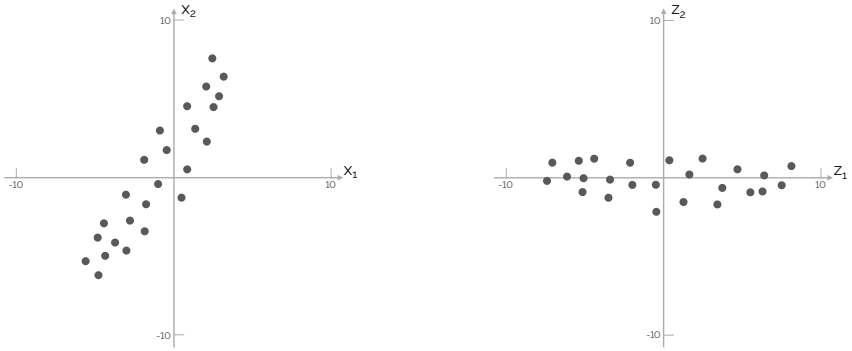

Figure 1.8. Original observations of the dataset (left) and their projection with respect to their PCs (right). The variation of the realisations is more significant in the direction of x_2 than x_1. Once projected with respect to their PCs, the variation is even more significant in the direction of z_1 than in either of the original variables, as it captures most of their variance. Graph adapted from [81].

The PCs are computed based on the covariance matrix of $\mathbf{x}$, $\boldsymbol{\Sigma}$. The diagonal of this matrix gives the variance of the i^{th} variable whereas the other elements give the covariance between the i^{th} and the j^{th} variables where $i \neq j$. Out of this matrix, $\boldsymbol{\alpha}_\mathbf{k}$ is the eigenvector of $\boldsymbol{\Sigma}$ corresponding to its k^{th} highest eigenvalue λ_k. Finally, as the $\boldsymbol{\alpha}_\mathbf{k}$ for all $k = 1, 2, \cdots, p$ are normalized, i.e. $\boldsymbol{\alpha}_\mathbf{k}{}^T\boldsymbol{\alpha}_\mathbf{k} = 1$, var $\left(z_k\right) = \lambda_k$, where var $\left(z_k\right)$

is the variance of z_k. In other words, α_{ki}, i.e. the components of$\boldsymbol{\alpha}_{\mathbf{k}}$, give the weight of the i^{th} original variable, x_i, in the k^{th} PC, i.e. z_k, where λ_k gives the variance of the original data captured by z_k. In other words, a high absolute value of α_{ki} means that x_i has a significant impact in the direction given by the k^{th} PC [82]. The interested reader is invited to refer to the work of Jolliffe [81] for further mathematical demonstrations, information and examples.

1.4.2 Principal components of the transition

As introduced, the objective is to define the main technological drivers of the variation through the transition to 2050 subject to uncertainties. To do so, before calculating the PCs of the transition, three preliminary steps are necessary: (i) data selection, (ii) data scaling and, (iii)outliers management. After this preprocessing, PCs can be computed for each of the year of the transition then aggregated to give a bigger picture over the whole transition.

Data selection

Prior to any data processing, the choice of the original dataset is fundamental. In the will to characterize the variations of design within the transition under uncertainties, we have focused on the installed capacities, $\mathbf{F}(y, j)$ for all $y \in YEARS$ and $j \in TECH$ (see Eq. 1.15). Even though these represent only a part of the result of the optimization, along with the operation, focusing on the installed capacities give a direct information regarding the required capital investment (see Eq. 1.8) and, more indirectly, the resources to use. In other words, it captures the technological landscape of the transition. Having defined the type of variable to consider, we need to assemble a relevant dataset. This is given by the runs to quantify the impact of the uncertain parameters on the total cost of transition required by the method described in Section 1.2. Overall, the original dataset is $\mathbf{x}(y, j, s)$ where, on top of y and j previously defined, $s \in [1, 2, ..., S]$ states for the sample number of the uncertainty quantification method. For the investigated case detailed in Chapter **??**, this represents $S = 240$ samples resulting from the perfect foresight optimization of the transition pathway under uncertainties. Finally, among the seven representative years of the transition, we do not consider 2020 as it is the initialisation year for which the design of the system is fixed, to be representative of the actual design that was in place (see Appendix **??**). In other words, we focus here only on the years 2025, 2030, 2035, 2040, 2045 and 2050. This gives the whole dataset considered in this PCA (see Figure 1.9).

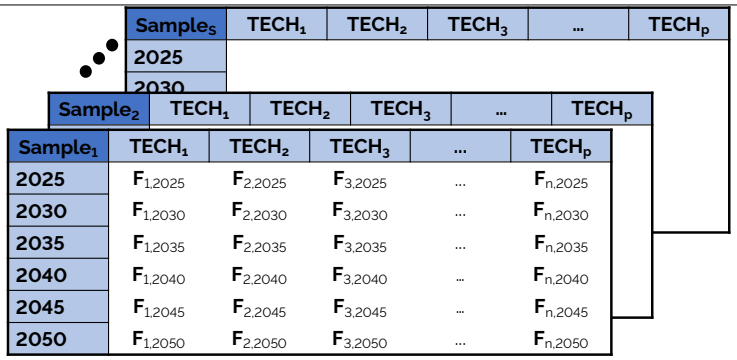

Sample$_1$	TECH$_1$	TECH$_2$	TECH$_3$	...	TECH$_p$
2025	$F_{1,2025}$	$F_{2,2025}$	$F_{3,2025}$	...	$F_{n,2025}$
2030	$F_{1,2030}$	$F_{2,2030}$	$F_{3,2030}$	...	$F_{n,2030}$
2035	$F_{1,2035}$	$F_{2,2035}$	$F_{3,2035}$	...	$F_{n,2035}$
2040	$F_{1,2040}$	$F_{2,2040}$	$F_{3,2040}$	...	$F_{n,2040}$
2045	$F_{1,2045}$	$F_{2,2045}$	$F_{3,2045}$	...	$F_{n,2045}$
2050	$F_{1,2050}$	$F_{2,2050}$	$F_{3,2050}$	...	$F_{n,2050}$

Figure 1.9. Original raw data considered in the Principal Component Analysis (PCA) of the variation of the design strategy through the transition, $\mathbf{x}(y, j, s)$.

Data scaling

Preprocessing the dataset before employing a method to reduce dimensionality, like PCA, can greatly affect the structure of the simplified representation and the characteristics of the features extracted from the dataset [83, 84]. Scaling the original raw data via normalization, i.e. reducing data to [0, 1] interval has a double purposes: to assess variables (i) representing different sorts of features, with different units (e.g. installed capacity of electricity and mobility technologies) and, (ii) ranging over the different orders of magnitude (e.g. installed capacity of private and public mobility) (see Appendix **??**). Consequently, the first part of this data preprocessing consists in scaling the installed capacities versus their respective sector and representative year (see Eq. 1.28). The sectors, as defined in EnergyScope, are the electricity, high-temperature (HT) heat, low-temperature (LT) heat, passenger mobility, freight mobility, non-energy demand (NED), storage and infrastructures. For instance, the installed capacity of PV panels in the year y of the sample s is scaled by the maximum installed capacity in the electricity sector in the year y among all the samples.

$$\mathbf{x}^*(y, j, s) = \frac{\mathbf{x}(y, j, s)}{\max_{sec,y}(\mathbf{x}(y, j, s))} \quad \forall y \in YEARS, sec \in SECTORS \tag{1.28}$$

Then, to give "directions/metrics" representative to the size of each sector within the energy system, we added another weight based on the relative share of commodity produced by each sector. For the case study of Belgium detailed in Chapter **??**, this gives a higher weight for electricity and low-temperature heat sectors (see Figure 1.10).

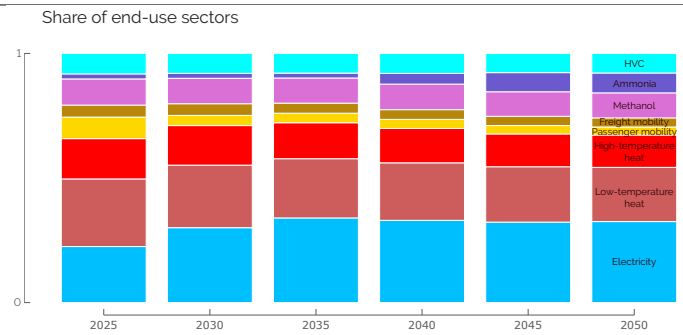

Figure 1.10. Multiplying factor for each of the end-use sectors in the case of Belgian energy transition. These shares are based on results of the reference scenario (REF) where nominal values are considered for the uncertain parameters and the transition is optimized through the perfect foresight approach. Over the transition, sectors like electricity or methanol become more important due to sector coupling, e.g. e-mobility or methanol-to-olefins (MTO).

To do so, we have arbitrarily considered these shares from the REF case, where the pathway is optimized according to the perfect foresight approach and considering all the uncertain parameters to their nominal value (see Chapter **??**). The end-use-demands as well as the commodity produced for the sector coupling are based on the results of this deterministic REF case. For instance, the share of the electricity sector accounts for its EUD and the electricity produced to supply other sectors (e.g. heat, mobility). Finally, to compare apples with apples, we converted the EUD in the mobility sectors, i.e. passenger and freight, into the ?? they require in the REF case. This gives the second weighing factor to scale data, on top of the one of Eq. 1.28 (see Eq. 1.29).

$$\mathbf{x}^{**}(y,j,s) = \mathbf{x}^{*}(y,j,s) \cdot \text{share}_{\text{EUD}}(y, sec) \quad \forall y \in YEARS, sec \in SECTORS \quad (1.29)$$

One would notice that this second scaling factor omits the infrastructure and storage technologies. In the process to define "metrics" to assess the robustness of a policy for the case of Belgium, this has a negligible impact. Indeed, the variation of the installed capacity of these technologies are either limited compared to end-use-type (EUT) technologies, i.e. limiting their influence in the definition of PCs, or directly linked to these EUT technologies (e.g. district heating network (DHN) installed capacity is directly proportional to technologies producing LT heat in DHN or the

additional capacity of grid is caused by additional capacities of VRES).

Outliers management

Handling outliers is one of the biggest challenges in data science [85]. These are defined as data points differing significantly from the rest of the data set. Being extreme values, outliers influence the overall dataset variance and, consequently, rotate the PCs directions towards them [86]. In the context of PCA, outliers could be defined as "model fit outliers" as their presence influences the fit of the model. There are several techniques to detect/define and handle the outliers [85]. In this work, detection is performed via the box plot technique, as outliers are identified as those points lying beyond the plot's whiskers, or fences. These whiskers are themselves constructed as being 1.5 times the interquatile range (IQR) (Q3 - Q1) higher or lower than the third (Q3) or first quartile (Q1), respectively (see Figure 1.11). Therefore, the installed capacity of a technology in the year *y* of the sample *s* is defined as an outlier if it falls out of this range compared to the rest of the dataset for this specific technology and year across all the samples. Then, one option to handle these outliers would be to remove the whole data point for which one technology presents an outlying installed capacity. However, it would lead to reducing the entire dataset (i.e. several thousands of points) to too few data points (i.e. several tens) limiting the applicability of the PCA approach. Consequently, we have decided to keep these points but carry out a modification of them [85]. In practice, the value of "high outliers" or "low outliers" is set to the upper or lower fence, respectively.

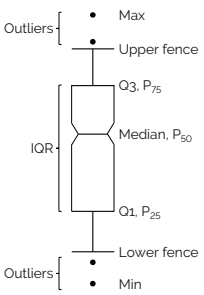

Figure 1.11

Principal components of each representative year

Now that data are selected and preprocessed, principal components are first computed for each representative year separately, using the Python package PCA from SKLEARN.DECOMPOSITION. As explained in Section 1.4.1, the number of PCs per year to retain can go up to the number of considered variables (i.e. 73[2] in our case study) which is intractable. Moreover, the first PCs keep track of most of the variance of the system whereas the last ones present a smaller interest. Choosing the appropriate threshold involves a trade-off. Retaining too few principal components may result

[2] 73 technologies out of the 113 in total as we do not consider the 15 infrastructure technologies nor the 25 storage technologies.

in loss of important information, while retaining too many may lead to over-fitting or computational inefficiency. The good practice followed in this work is to compute, for each of the representative years of the transition (except 2020), the PCs that capture 90% of the total variance of this year [81]. At the end of this step, we have a list of m PCs, i.e. $\mathrm{PC}_{y,i}$ where y stands for the year between 2025 and 2050 and

$$\sum_{i=0}^{m} \mathrm{var}\left(\mathrm{PC}_{y,i}\right) \geq 90\% \sum_{i=0}^{p} \mathrm{var}\left(\mathrm{PC}_{y,i}\right) \quad \forall y \in \mathit{YEARS} \tag{1.30}$$

where m is presumably different for each representative year and p is the total number of variables, hence the maximum number of PCs. For the entire transition, it gives a total of M $\mathrm{PC}_{y,i}$.

Principal components of the transition

The final step consists in defining metrics on the whole transition based on the $\mathrm{PC}_{y,i}$ computed for each representative year, separately. To do so, all the $\mathrm{PC}_{y,i}$ from every year are sorted together in a descending order based on their respective variance. Then, starting with the one with the highest absolute variance, all the other $\mathrm{PC}_{y,i}$ similar to it are clustered together. The similarity between two PCs is defined according to the cosine similarity approach. Indeed, as detailed in Section 1.4.1, a PC represents a vector for which the components are related to each variable of interest. Therefore, in this work, PCs are considered similar if their cosine similarity, $S_C(A, B)$, is greater or equal to 90%:

$$S_C(A, B) := \cos(\theta) = \frac{\mathbf{A} \cdot \mathbf{B}}{\|\mathbf{A}\|\|\mathbf{B}\|} = \frac{\sum_{i=1}^{n} A_i B_i}{\sqrt{\sum_{i=1}^{n} A_i^2} \cdot \sqrt{\sum_{i=1}^{n} B_i^2}} \geq 90\% \tag{1.31}$$

where A and B represent two different PCs. The components of these similar PCs are then averaged to form the first PC of the transition, $\mathrm{PC}_{\mathrm{transition},1}$. Then, the process repeats with the $\mathrm{PC}_{y,i}$ with the highest absolute variance but that has not been integrated in the construction of $\mathrm{PC}_{\mathrm{transition},1}$, to form $\mathrm{PC}_{\mathrm{transition},2}$. This goes on until the sum of the absolute variance of the N $\mathrm{PC}_{y,i}$ used to construct these $\mathrm{PC}_{\mathrm{transition}}$ is greater or equal to 90% of the sum of the absolute variance of all the M $\mathrm{PC}_{y,i}$ generated at the previous step:

$$\sum_{i=0}^{N} \text{var}\left(\text{PC}_{y,i}\right) \geq 90\% \sum_{i=0}^{M} \text{var}\left(\text{PC}_{y,i}\right) \tag{1.32}$$

Robustness assessment of roadmaps

Similarly to the work of Moret et al. [53], roadmaps are defined by setting minimal installed capacities based on the results of different transition pathway optimizations (see Chapter **??**). The $\text{PC}_{\text{transition}}$ are the "direction/metrics" on which are projected the results from the myopic pathway optimization subject to minimal installed capacities set by these roadmaps. In conclusion, a roadmap would be defined as more robust than another one if the projection of its myopic runs on the different $\text{PC}_{\text{transition}}$ span on a more narrow range.

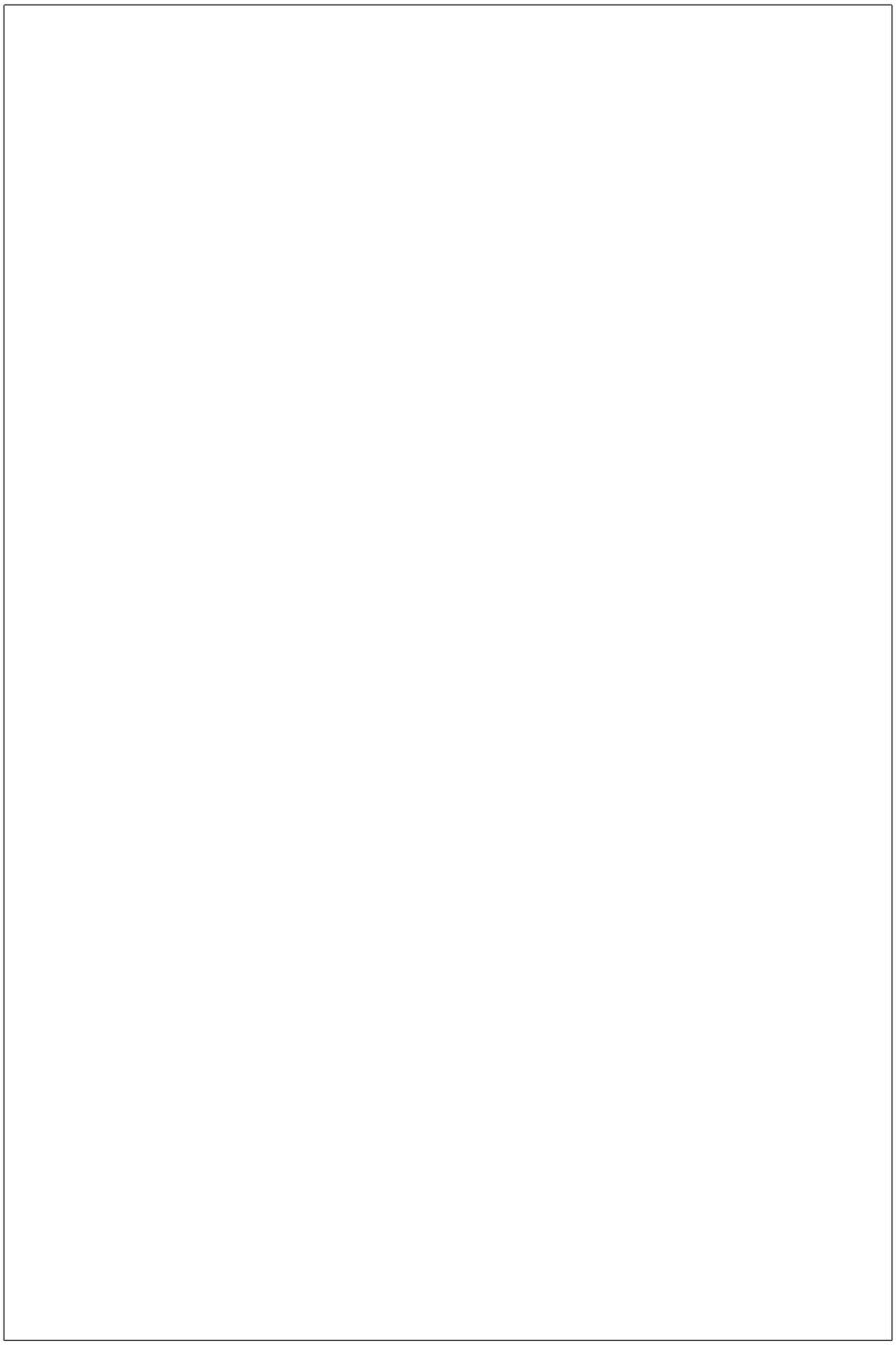

Bibliography

[1] Intergovernmental Pael on Climate Change (IPCC), Global Warming of 1.5°C. An IPCC Special Report on the impacts of global warming of 1.5°C above pre-industrial levels and related global greenhouse gas emission pathways, in the context of strengthening the global response to the threat of climate change, sustainable development, and efforts to eradicate poverty, Technical Report, 2018.

[2] Y. Kaya, K. Yokobori, et al., Environment, energy, and economy: strategies for sustainability, volume 4, United Nations University Press Tokyo, 1997.

[3] IPCC, Emissions Scenarios, Technical Report, Intergovernmental Panel on Climate Change, 2000.

[4] J. C. Dodson, P. Dérer, P. Cafaro, F. Götmark, Population growth and climate change: Addressing the overlooked threat multiplier, Science of the Total Environment 748 (2020) 141346.

[5] N. Scovronick, M. B. Budolfson, F. Dennig, M. Fleurbaey, A. Siebert, R. H. Socolow, D. Spears, F. Wagner, Impact of population growth and population ethics on climate change mitigation policy, Proceedings of the National Academy of Sciences 114 (2017) 12338–12343.

[6] IPCC, Climate Change 2022: Mitigation of Climate Change - Summary for Policymakers, Technical Report, Intergovernmental Panel on Climate Change, 2022.

[7] J. Lage, J. Thema, C. Zell-Ziegler, B. Best, L. Cordroch, F. Wiese, Citizens call for sufficiency and regulation—a comparison of european citizen assemblies and national energy and climate plans, Energy Research & Social Science 104 (2023) 103254.

[8] D. W. O'Neill, A. L. Fanning, W. F. Lamb, J. K. Steinberger, A good life for all within planetary boundaries, Nature sustainability 1 (2018) 88–95.

[9] S. Schmidt, H. Weigt, Interdisciplinary energy research and energy consumption: what, why, and how?, Energy Research & Social Science 10 (2015) 206–219.

[10] European Parliament, Directive (EU) 2023/2413 of the European Parliament and of the Council of 18 October 2023 amending Directive (EU) 2018/2001, Regulation (EU) 2018/1999 and Directive 98/70/EC as regards the promotion of energy from renewable sources, and repealing Council Directive (EU) 2015/652, Technical Report, European Parliament, 2023. Official Journal of the European Union 2413, 1-77.

[11] International Energy Agency, World energy outlook 2019, `https://www.iea.org/reports/world-energy-outlook-2019`, 2020.

[12] E. Rozzi, F. D. Minuto, A. Lanzini, P. Leone, Green synthetic fuels: Renewable routes for the conversion of non-fossil feedstocks into gaseous fuels and their end uses, Energies 13 (2020) 420.

[13] W. L. Ahlgren, The dual-fuel strategy: An energy transition plan, Proceedings of the IEEE 100 (2012) 3001–3052. doi:`10.1109/JPROC.2012.2192469`.

[14] C. Lhuillier, P. Brequigny, F. Contino, C. Mounaïm-Rousselle, Experimental study on ammonia/hydrogen/air combustion in spark ignition engine conditions, Fuel 269 (2020) 117448.

[15] M. Pochet, H. Jeanmart, F. Contino, A 22: 1 compression ratio ammonia-hydrogen hcci engine: Combustion, load, and emission performances, Frontiers in Mechanical Engineering 6 (2020) 43.

[16] M. Robinius, A. Otto, P. Heuser, L. Welder, K. Syranidis, D. S. Ryberg, T. Grube, P. Markewitz, R. Peters, D. Stolten, Linking the power and transport sectors—part 1: The principle of sector coupling, Energies 10 (2017) 956.

[17] T. W. Brown, T. Bischof-Niemz, K. Blok, C. Breyer, H. Lund, B. V. Mathiesen, Response to 'burden of proof: A comprehensive review of the feasibility of 100% renewable-electricity systems', Renewable and sustainable energy reviews 92 (2018) 834–847.

[18] G. Limpens, H. Jeanmart, System lcoe: applying a whole-energy system model to estimate the integration costs of photovoltaic, in: 34th International Conference on Efficiency, Cost, Optimization, Simulation and Environmental Impact of Energy Systems (ECOS 2021). Taormina, Italy, 2021.

[19] T. Brown, D. Schlachtberger, A. Kies, S. Schramm, M. Greiner, Synergies of sector coupling and transmission reinforcement in a cost-optimised, highly renewable european energy system, Energy 160 (2018) 720–739.

[20] H. Stančin, H. Mikulčić, X. Wang, N. Duić, A review on alternative fuels in future energy system, Renewable and Sustainable Energy Reviews 128 (2020). doi:10.1016/j.rser.2020.109927.

[21] K. Verleysen, D. Coppitters, A. Parente, W. De Paepe, F. Contino, How can power-to-ammonia be robust? Optimization of an ammonia synthesis plant powered by a wind turbine considering operational uncertainties, Fuel 266 (2020) 117049.

[22] R. Rosa, The Role of Synthetic Fuels for a Carbon Neutral Economy, C 3 (2017) 11. doi:10.3390/c3020011.

[23] M. Child, D. Bogdanov, C. Breyer, The role of storage technologies for the transition to a 100% renewable energy system in europe, Energy Procedia 155 (2018) 44–60.

[24] V. Dias, M. Pochet, F. Contino, H. Jeanmart, Energy and economic costs of chemical storage, Frontiers in Mechanical Engineering 6 (2020) 21.

[25] M. Millinger, P. Tafarte, M. Jordan, A. Hahn, K. Meisel, D. Thrän, Electrofuels from excess renewable electricity at high variable renewable shares: cost, greenhouse gas abatement, carbon use and competition, Sustainable Energy & Fuels 5 (2021) 828–843.

[26] S. Horvath, M. Fasihi, C. Breyer, Techno-economic analysis of a decarbonized shipping sector: Technology suggestions for a fleet in 2030 and 2040, Energy Conversion and Management 164 (2018) 230–241.

[27] S. Brynolf, M. Taljegard, M. Grahn, J. Hansson, Electrofuels for the transport sector: A review of production costs, Renewable and Sustainable Energy Reviews 81 (2018) 1887–1905.

[28] J. Mertens, R. Belmans, M. Webber, Why the carbon-neutral energy transition will imply the use of lots of carbon, C—Journal of Carbon Research 6 (2020) 39.

[29] Institute for Sustainable Process Technology, Power to Ammonia (2017). URL: http://www.ispt.eu/media/ISPT-P2A-Final-Report.pdf.

[30] B. V. Mathiesen, H. Lund, D. Connolly, H. Wenzel, P. A. Østergaard, B. Möller, S. Nielsen, I. Ridjan, P. Karnøe, K. Sperling, et al., Smart energy systems for coherent 100% renewable energy and transport solutions, Applied Energy 145 (2015) 139–154.

[31] Y. Zeng, Y. Cai, G. Huang, J. Dai, A review on optimization modeling of energy systems planning and ghg emission mitigation under uncertainty, Energies 4 (2011) 1624–1656.

[32] X. Yue, S. Pye, J. DeCarolis, F. G. Li, F. Rogan, B. Ó. Gallachóir, A review of approaches to uncertainty assessment in energy system optimization models, Energy strategy reviews 21 (2018) 204–217.

[33] S. Moret, V. Codina Gironès, M. Bierlaire, F. Maréchal, Characterization of input uncertainties in strategic energy planning models, Applied Energy 202 (2017) 597–617.

[34] S. Pfenninger, A. Hawkes, J. Keirstead, Energy systems modeling for twenty-first century energy challenges, Renewable and Sustainable Energy Reviews 33 (2014) 74–86.

[35] F. Y. Kuo, I. H. Sloan, Lifting the curse of dimensionality, Notices of the AMS 52 (2005) 1320–1328.

[36] United Nations, The 17 goals, `https://sdgs.un.org/goals`, September 2015 (accessed June 7, 2023).

[37] G. Limpens, Generating energy transition pathways: application to Belgium, Ph.D. thesis, Université Catholique de Louvain, 2021.

[38] E. Guevara, F. Babonneau, T. Homem-de Mello, Modeling uncertainty processes for multi-stage optimization of strategic energy planning: An auto-regressive and markov chain formulation (2022).

[39] G. Limpens, D. Coppitters, X. Rixhon, F. Contino, H. Jeanmart, The impact of uncertainties on the belgian energy system: Application of the polynomial chaos expansion to the energyscope model, Proceedings of the ECOS (2020).

[40] X. Rixhon, G. Limpens, D. Coppitters, H. Jeanmart, F. Contino, The role of electrofuels under uncertainties for the belgian energy transition, Energies 14 (2021) 4027.

[41] B. Goffaux, Pathway towards energy sustainability in belgium under uncertainties, 2021. URL: https://dial.uclouvain.be/memoire/ucl/object/thesis:30574.

[42] S. Moret, M. Bierlaire, F. Maréchal, Strategic energy planning under uncertainty: a mixed-integer linear programming modeling framework for large-scale energy systems, in: Computer Aided Chemical Engineering, volume 38, Elsevier, 2016, pp. 1899–1904.

[43] G. Limpens, S. Moret, H. Jeanmart, F. Maréchal, Energyscope td: A novel open-source model for regional energy systems, Applied Energy 255 (2019) 113729.

[44] G. Limpens, X. Rixhon, F. Contino, H. Jeanmart, Energyscope pathway: an open-source model to optimise the energy transition pathways of a regional whole-energy system, Elsevier in Applied Energy 358 (2024). doi:https://doi.org/10.1016/j.apenergy.2023.122501.

[45] D. Coppitters, Robust design optimization of hybrid renewable energy systems, Vrije Universiteit Brussel (VUB), University of Mons (UMONS), Mons (2021).

[46] G. Limpens, EnergyScope Pathway documentation, Accessed 2022. URL: https://energyscope-pathway.readthedocs.io/en/v1.1/.

[47] T. Stocker, Climate change 2013: the physical science basis: Working Group I contribution to the Fifth assessment report of the Intergovernmental Panel on Climate Change, Cambridge university press, 2014.

[48] J. Schnidrig, J. Brun, F. Maréchal, M. Margni, Integration of life cycle impact assessment in energy system modelling, Proceedings of ECOS 2023 (2023).

[49] S. Babrowski, T. Heffels, P. Jochem, W. Fichtner, Reducing computing time of energy system models by a myopic approach: A case study based on the perseus-net model, Energy systems 5 (2014) 65–83.

[50] K. Poncelet, E. Delarue, D. Six, W. D'haeseleer, Myopic optimization models for simulation of investment decisions in the electric power sector, in: 2016 13th International Conference on the European Energy Market (EEM), IEEE, 2016, pp. 1–9.

[51] F. F. Nerini, I. Keppo, N. Strachan, Myopic decision making in energy system decarbonisation pathways. a uk case study, Energy strategy reviews 17 (2017) 19–26.

[52] C. F. Heuberger, I. Staffell, N. Shah, N. Mac Dowell, Impact of myopic decision-making and disruptive events in power systems planning, Nature Energy 3 (2018) 634–640.

[53] S. Moret, F. Babonneau, M. Bierlaire, F. Maréchal, Overcapacity in european power systems: Analysis and robust optimization approach, Applied Energy 259 (2020) 113970.

[54] AMPL Optimization Inc., AMPL Python API, `https://amplpy.ampl.com/en/latest/`, 2024.

[55] V. Krey, Vergleich kurz-und langfristig ausgerichteter optimierungsansätze mit einem multi-regionalen energiesystemmodell unter berücksichtigung stochastischer parameter (2006).

[56] G. Mavromatidis, K. Orehounig, J. Carmeliet, Uncertainty and global sensitivity analysis for the optimal design of distributed energy systems, Applied Energy 214 (2018) 219–238.

[57] J. Peace, J. Weyant, Insights not numbers: the appropriate use of economic models, White paper of Pew Center on Global Climate Change (2008).

[58] C. Marnay, A. S. Siddiqui, Addressing an uncertain future using scenario analysis, Lawrence Berkeley National Laboratory, 2006.

[59] X. Li, S. Moret, F. Baldi, F. Maréchal, Are renewables really that expensive? the impact of uncertainty on the cost of the energy transition, in: Computer Aided Chemical Engineering, volume 46, Elsevier, 2019, pp. 1753–1758.

[60] D. Coppitters, W. De Paepe, F. Contino, Robust design optimization of a photovoltaic-battery-heat pump system with thermal storage under aleatory and epistemic uncertainty, Energy 229 (2021) 120692.

[61] Hydrogen Import Coalition, Shipping sun and wind to Belgium is key in climate neutral economy, `https://www.portofantwerp.com/sites/default/files/Hydrogen%20Import%20Coalition.pdf`, 2021.

[62] D. Coppitters, W. De Paepe, F. Contino, Robust design optimization and stochastic performance analysis of a grid-connected photovoltaic system with battery storage and hydrogen storage, Energy 213 (2020) 118798.

[63] D. Coppitters, P. Tsirikoglou, W. D. Paepe, K. Kyprianidis, A. Kalfas, F. Contino, RHEIA: Robust design optimization of renewable Hydrogen and dErIved energy cArrier systems, Journal of Open Source Software 7 (2022) 4370. doi:10.21105/joss.04370.

[64] D. Coppitters, RHEIA documentation, Accessed 2022. URL: https://rheia.readthedocs.io/en/latest/index.html.

[65] B. Sudret, Polynomial chaos expansions and stochastic finite element methods, Risk and reliability in geotechnical engineering (2014) 265–300.

[66] P. Bratley, B. Fox, Implementing sobols quasirandom sequence generator (algorithm 659), ACM Transactions on Mathematical Software 29 (2003) 49–57.

[67] M. D. Morris, Factorial Sampling Plans for Preliminary Computational Experiments, Technometrics 33 (1991) 161–174.

[68] G. Sin, K. V. Gernaey, Improving the morris method for sensitivity analysis by scaling the elementary effects, in: Computer Aided Chemical Engineering, volume 26, Elsevier, 2009, pp. 925–930.

[69] S. Moret, Strategic energy planning under uncertainty, Ph.D. thesis, EPFL, 2017.

[70] D. Cao, W. Hu, J. Zhao, G. Zhang, B. Zhang, Z. Liu, Z. Chen, F. Blaabjerg, Reinforcement learning and its applications in modern power and energy systems: A review, Journal of modern power systems and clean energy 8 (2020) 1029–1042.

[71] R. S. Sutton, A. G. Barto, Reinforcement learning: An introduction, MIT press, 2018.

[72] David Silver, RL Course by David Silver, https://www.youtube.com/watch?v=2pWv7GOvuf0&list=PLzuuYNsE1EZAXYR4FJ75jcJseBmo4KQ9-, 2016.

[73] A. Perera, P. Kamalaruban, Applications of reinforcement learning in energy systems, Renewable and Sustainable Energy Reviews 137 (2021) 110618.

[74] T. Haarnoja, A. Zhou, P. Abbeel, S. Levine, Soft actor-critic: Off-policy maximum entropy deep reinforcement learning with a stochastic actor, in: International conference on machine learning, PMLR, 2018, pp. 1861–1870.

[75] T. Haarnoja, H. Tang, P. Abbeel, S. Levine, Reinforcement learning with deep energy-based policies, in: International conference on machine learning, PMLR, 2017, pp. 1352–1361.

[76] B. D. Ziebart, Modeling purposeful adaptive behavior with the principle of maximum causal entropy, Carnegie Mellon University, 2010.

[77] A. Raffin, A. Hill, A. Gleave, A. Kanervisto, M. Ernestus, N. Dormann, Stable-baselines3: Reliable reinforcement learning implementations, The Journal of Machine Learning Research 22 (2021) 12348–12355.

[78] M. Abadi, A. Agarwal, P. Barham, E. Brevdo, Z. Chen, C. Citro, G. S. Corrado, A. Davis, J. Dean, M. Devin, et al., Tensorflow: Large-scale machine learning on heterogeneous distributed systems, arXiv preprint arXiv:1603.04467 (2016).

[79] K. Pearson, On lines and planes of closest fit to systems of points in space., The London, Edinburgh, and Dublin philosophical magazine and journal of science 2 (1901) 559–572.

[80] H. Hotelling, Analysis of a complex of statistical variables into principal components., Journal of educational psychology 24 (1933) 417.

[81] I. T. Jolliffe, Principal component analysis for special types of data, Springer, 2002.

[82] K. Zdybał, G. D'Alessio, G. Aversano, M. R. Malik, A. Coussement, J. C. Sutherland, A. Parente, Advancing reacting flow simulations with data-driven models, arXiv preprint arXiv:2209.02051 (2022).

[83] A. Parente, J. C. Sutherland, Principal component analysis of turbulent combustion data: Data pre-processing and manifold sensitivity, Combustion and flame 160 (2013) 340–350.

[84] K. Peerenboom, A. Parente, T. Kozák, A. Bogaerts, G. Degrez, Dimension reduction of non-equilibrium plasma kinetic models using principal component analysis, Plasma Sources Science and Technology 24 (2015) 025004.

[85] H. Aguinis, R. K. Gottfredson, H. Joo, Best-practice recommendations for defining, identifying, and handling outliers, Organizational research methods 16 (2013) 270–301.

[86] I. Stanimirova, M. Daszykowski, B. Walczak, Dealing with missing values and outliers in principal component analysis, Talanta 72 (2007) 172–178.